AD 262319

UNITED STATES
NAVAL POSTGRADUATE SCHOOL

61-4-4

XEROX

THESIS

THE INFLUENCE OF WINDS AND RELATIVE HUMIDITY ON THE SEASONAL THERMOCLINE AT OCEAN STATION "P"

* * * * *

Marion J. Clark

Lieutenant, United States Navy

THE INFLUENCE OF WINDS AND RELATIVE HUMIDITY ON THE SEASONAL THERMOCLINE AT OCEAN STATION "P"

* * * * * * *

Marion J. Clark

THE INFLUENCE OF WINDS AND RELATIVE HUMIDITY ON THE SEASONAL THERMOCLINE AT OCEAN STATION "P"

* * * * *

Marion J. Clark

1 9 6 1

UNITED STATES NAVAL POSTGRADUATE SCHOOL

Degree: Master of Science in Meteorology

Classification:

Thesis: Unclassified

Abstract: Unclassified

Title of Thesis: Unclassified

Contains no proprietary information

THE INFLUENCE OF WINDS AND RELATIVE HUMIDITY ON THE SEASONAL THERMOCLINE AT OCEAN STATION "P"

by

Marion J. Clark

This work is accepted as fulfilling the thesis requirements for the degree of

MASTER OF SCIENCE

IN

METEOROLOGY

from the

United States Naval Postgraduate School

Faculty Advisor

Chairman, Department of Meteorology and Oceanography

Approved:

Academic Dean

THE INFLUENCE OF WINDS AND RELATIVE HUMIDITY ON THE SEASONAL THERMOCLINE AT OCEAN STATION "P"

by

Marion J. Clark

Lieutenant, United States Navy

Submitted in partial fulfillment of
the requirements for the degree of

MASTER OF SCIENCE

IN

METEOROLOGY

United States Naval Postgraduate School

Monterey, California

1961

ABSTRACT

The ability to predict the temperature structure successfully in the upper layers of the ocean has long been sought by both military and civilian scientists, with prime interest to date being focused on obvious surface meteorological parameters, such as air-sea temperature difference and wind speed. In an attempt to approach the problem from a different viewpoint, attention in this paper has been directed to the higher atmospheric layers and such significant conditions aloft which may possibly be associated with variations in the temperature structure in the ocean. Primary interest has been in the onset and initial disturbances or 'sinkings' of the newly-established seasonal thermocline at ocean station "P" (latitude 50N, longitude 145W).

One of the main objectives of this paper is to detect significant meteorological changes or disturbances in the state of the atmosphere which accompany or precede distinct variations in the thermocline; and, if possible, to take advantage of these atmospheric changes as possible forecasting tools to predict the temperature structure of the upper layers of the ocean or the depth of the mixed layer.

As a result of this investigation, two basic hypotheses are presented: (1) that the ocean upper mixed layer and the layer of air in immediate contact with the ocean surface should be treated as a unit which is affected by meteorological parameters above this unit aloft, and (2) that there exists in the upper atmosphere a 'mirror image'

level where the fluctuations in the wind speed closely depict the oscillation in the depth of the mixed layer.

In support of this theory, profiles and graphs of meteorological parameters such as temperature, wind speed and relative humidity have been prepared for various levels in the atmosphere. A synoptic technique for predicting the annual commencement date of the seasonal thermocline using temperature and wind discontinuities aloft is presented. In addition, a mathematical relationship between wind speed aloft and the depth of the mixed layer has been developed in support of hypothesis (2) with tested predictions included as Appendix I. The complete investigation, results and conclusions drawn, are based on data obtained at ocean station "P".

For his invaluable aid in the preparation of this manuscript, the author is deeply indebted to Associate Professor G. H. Jung, Department of Meteorology and Oceanography, U.S. Naval Postgraduate School, Monterey.

TABLE OF CONTENTS

LIST OF ILLUSTRATIONS

1. Introduction.

Modern technological developments continue to accelerate man's exploration of both outer space and the depths of the oceans; scientific curiosity continues to lead him further and further from his native environment, the face of the earth; hence it becomes increasingly necessary, and indeed vital, that our knowledge of these newly invaded mediums be expanded.

The study of the oceans is a challenging one. Although oceanographers have accomplished a great deal toward successfully unravelling the age-old mysteries of the deep, there still remains much to be learned in this area. Indeed, this is one field where modern technology has far surpassed our limited knowledge of the physical and dynamical properties of the transporting medium. For example, sonar has been developed to a high degree of sophistication, yet its operational use is limited by lack of knowledge concerning the temperature distribution in the sea.

The ability to predict the temperature structure successfully in the upper layers of the ocean has long been sought by both military and civilian scientists. Numerous approaches to the problem, both subjective and objective in nature, have been made, yet the fact remains that the temperature distribution in an extensive ocean layer encompassing approximately 70% of the earth's surface cannot be correctly forecast within the desired limits. However, if one takes into account the vast number of meteorological and oceanographical parameters, which are constantly

interacting at the air-sea interface and affecting the resultant ocean temperature structure beneath, it is not surprising that an immediate solution to this intricate problem has not been forthcoming.

Laevastu [1], in compiling a list of factors affecting the temperature of the surface layer of the sea, has listed over one hundred parameters which individually or collectively play some role in determining the temperature of the ocean. Relative humidity, wind speed, conduction of sensible heat, turbulence, incoming solar radiation, latent heat of evaporation, tidal currents and cloud cover are but a few of the important factors which must be considered. It is readily evident, then, that an accurate mathematical formulation of the problem would necessarily be a lengthy and complicated series of interacting terms requiring access to high speed computers for ready solution even after the basic form of the relationship had been prepared.

To date, in attempting to arrive at a more comprehensive understanding of the various reactions taking place at the air-sea interface, most research activity has been focused on the ocean surface or in the layer of air immediately adjacent to the surface. Many forecasting techniques involving obvious surface meteorological parameters such as relative humidity, air-sea temperature difference, wind speed, etc., have been offered but we still lack an accurate forecasting procedure which will correctly predict the temperature structure of the ocean's surface layers.

Undoubtedly such a forecasting technique will

eventually emerge; in the interim, in an attempt to approach the problem from a different viewpoint, attention in this paper has been directed to the higher atmospheric layers and such significant conditions aloft which may possibly be associated with large-scale variations in the temperature structure in the ocean. In other words, a synoptic approach to the problem has been attempted, closely associated with the synoptic approach used in meteorological forecasting. Primary interest has been in the onset and initial disturbances or 'sinkings' of the newly-established seasonal thermocline. One of the main objectives of this paper is to detect significant meteorological changes or disturbances in the state of the atmosphere which accompany or precede distinct variations in the thermocline; and, if possible, to take advantage of these atmospheric changes as possible forecasting tools to predict the temperature structure of the upper layers of the ocean or the depth of the mixed layer.

Profiles and graphs of meteorological parameters such as temperature, wind speed and relative humidity have been prepared for various levels in the atmosphere and are discussed in the body of the paper. A synoptic technique for predicting the annual commencement date of the seasonal thermocline using temperature and wind discontinuities aloft is also presented. In addition, a mathematical relationship between wind speed aloft and the depth of the mixed layer has been developed. Computed predictions and results for spring and summer months, 1956 through 1959,

are tabulated in Appendix I.

The complete investigation, results and conclusions drawn, are based on data obtained at Ocean Station "P" (latitude 50N, longitude 145W).

2. Background

The decision to approach this problem from a synoptic viewpoint, and to focus attention on the upper atmospheric levels rather than on the sea surface, was based on the results obtained and observations noted in two earlier papers prepared using data obtained at ocean station "J".

In the first paper [2], which was primarily a case history of the state of the atmosphere during the onset of the seasonal thermocline for the year 1959, four interesting phenomena were observed: (1) an abrupt horizontal wind discontinuity at 6000 meters preceded the first sudden 'sinking' of the newly-established thermocline; (2) a definite period of increased stability in the lower stratosphere preceded the chain-like reaction of temporary stability down through the atmospheric layers and culminated in increased surface wind speed and subsequent sudden sinking of the mixed layer (deepening of the isothermal ocean layer); (3) abrupt reversals of the stability distribution aloft coincided with the onset and sudden increases in depth of the mixed layer; and (4) expected variations in the relative humidity could be detected more readily at 850 mb than at the ocean surface.

Frawley and Clark [3], in attempting to construct a technique for determining the thermal structure in the upper layers of the ocean, considered various combinations of meteorological parameters and discovered that the inclusion of atmospheric stability gave the best results.

> Since....., the air-sea temperature difference for the 0200Z forecast did not seem adequate to describe the radiation effects, other meteorological parameters involving radiation effects were investigated. It was found that the best results were obtained by using the lapse rate through the layer 850 mb to 700 mb.

In reviewing the results summarized above, it was considered that sufficient justification existed for additional research in the higher atmospheric levels rather than on the level adjacent to the sea.

3. A Synoptic Technique for Determining the Annual Onset Date of the Seasonal Thermocline

First of all, consider the general state of the atmosphere aloft prior to the annual onset of the seasonal thermocline. In the 1958 spring edition of the Pan American Airways Technical Report [4], a statistical summary of seasonal incidences of jet stream centrums was compiled, based on ten years of hemispheric data. Station "P" is located in the area of maximum jet stream incidence in the Pacific Ocean, reported in [4], with the winter maximum dominating. It was found:

> Actually the increase of incidence in the spring over winter between 50N and 55N is somewhat misleading inasmuch as a high proportion of these incidences occur during March and can be considered as a carry-over from the winter patterns.

Analyzing the seasonal picture and tracing the gradient of maximum jet incidence throughout the spring months one notes the following trend: in March, prior to the establishment of the seasonal thermocline, maximum jet activity occurs directly aloft. However, during April and May there is a marked decrease in cyclonic activity and a marked decrease in the gradient of incidence of jet centrums. The seasonal thermocline commences during this period: and, for the balance of the spring and summer months, ridging, blocking and stable conditions predominate. As a result of the Pan American survey it is noted that:

> Pronounced decreases in incidence occur in April and May reflecting the greater frequency of ridging and blocking activity during these months...in the change from spring to summer the cyclone frequency between 50N and 55N diminishes which fact is well reflected in the decrease in jet stream count in this area.

It would therefore appear, on a very broad scale, that one of the prerequisites for 'setting the state' for the onset of the seasonal thermocline is the northward migration of the jet stream past station "P" during the early spring months. In support of this theory, it is noted that in all four years analyzed, a period of decreasing wind speed at the 500-mb level precedes the actual onset date.

In 1959 the seasonal thermocline commenced on 17 April. Before this date the winds at all levels were relatively light, varying in magnitude from twenty to forty knots, and they were primarily zonal in character. This zonal characteristic persisted during the period that the thermocline was being established at a depth of eight to ten meters. The first interruption to the pattern occurred eight days after the onset date. At this time, a decided wind discontinuity appeared at a level of 6000 meters (i.e., a sudden veering of 80° in wind direction) and exactly twenty hours later the first sudden sinking of the mixed layer occurred, a drop to a depth of forty-five meters.

This discontinuity could be readily tracked, with appropriate time lag, through higher tropospheric layers, across the tropopause and into the lower stratosphere. A surface front was located in the vicinity of station "P" and possessed the correct magnitude of slope to account for this discontinuity. However, the existence of a frontal passage is eliminated as the prime cause of the discontinuity if one concurs with the current belief that air-mass discontinuities do not extend into the stratosphere.

In an attempt to establish what role, if any, this upper level wind discontinuity played in the establishment and subsequent sinking of the thermocline, additional years were examined and the following observations noted: In 1958 the thermocline commenced on 15 May. Again, on 23 May, eight days after the actual commencement date, and following a period of relatively light zonal winds, the same discontinuity or veering of 80° in wind direction appears at 6000 meters. Also, twenty hours later, occurs the first sudden sinking of the mixed layer to a depth of forty-five meters.

At this point in the investigation, the possibility of utilizing the wind discontinuity aloft as a synoptic forecasting index was considered. In order to test this theory, the year 1956 was analyzed, and again, a major wind discontinuity was found at 6000 meters eight days after the onset date. In addition, twenty hours later the first sudden sinking of the mixed layer occurred. This consistency in the order of events suggested one set of criteria for establishing the sinking of the seasonal thermocline.

Temperature profiles, as illustrated in figures 1 and 2, were then drawn for three atmospheric levels: 500 mb, 850 mb and the surface. In all four years analyzed (1956-1959), it was noted that a relatively cold period immediately preceded the thermocline onset and that the 500 mb and 850 mb levels showed an abrupt increase in temperature, reaching maximum values on the actual onset date. This temperature maximum could be traced down through the atmosphere and it was interesting to note that the surface

temperature did not reach its maximum value until after the thermocline had set in and been well-established.

To summarize: the temperature maximum at 500 mb occurs on the thermocline onset date, and the wind discontinuity at 6000 meters eight days later occurs twenty hours before the first sudden sinking of the mixed layer depth. This combination of events is suggested as a synoptic forecasting technique for determining the commencement date of the seasonal thermocline and the first major sinking of the mixed layer.

In order to test this synoptic technique for 1961, daily wind and temperature data received from station "I" are being analyzed as of this writing and a prediction date for the 1961 thermocline onset will be forecast.

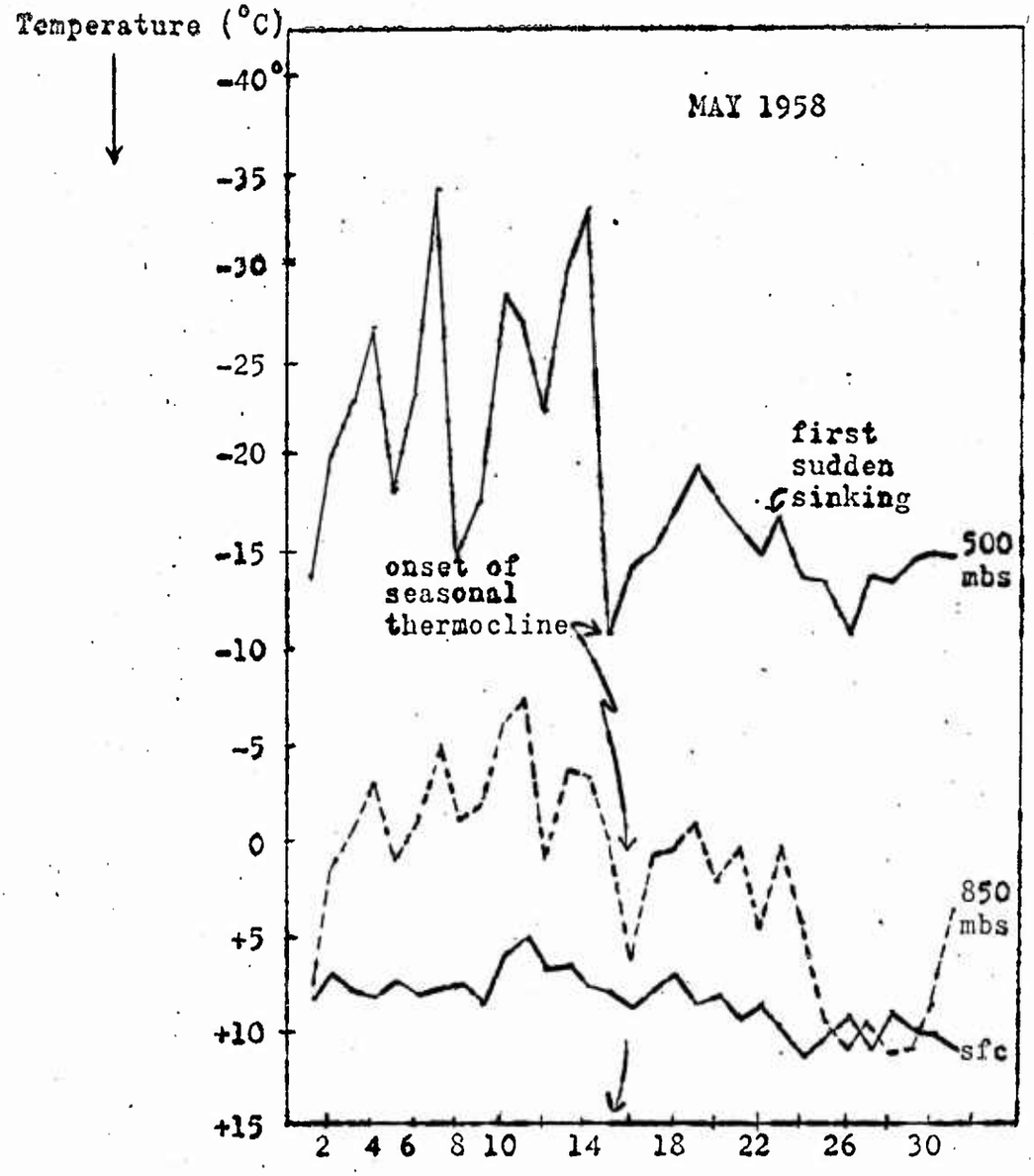

Fig. 1 Temperature profiles (0000Z) during the onset of the seasonal thermocline at Ocean Station "P". The 500 mb temperature reached a maximum on 15 May 1958, the date that the seasonal thermocline commenced. The date of maximum temperature can be traced down through the atmospheric layers with appropriate lag. Note that the surface temperature does not reach its maximum value until the thermocline is firmly established.

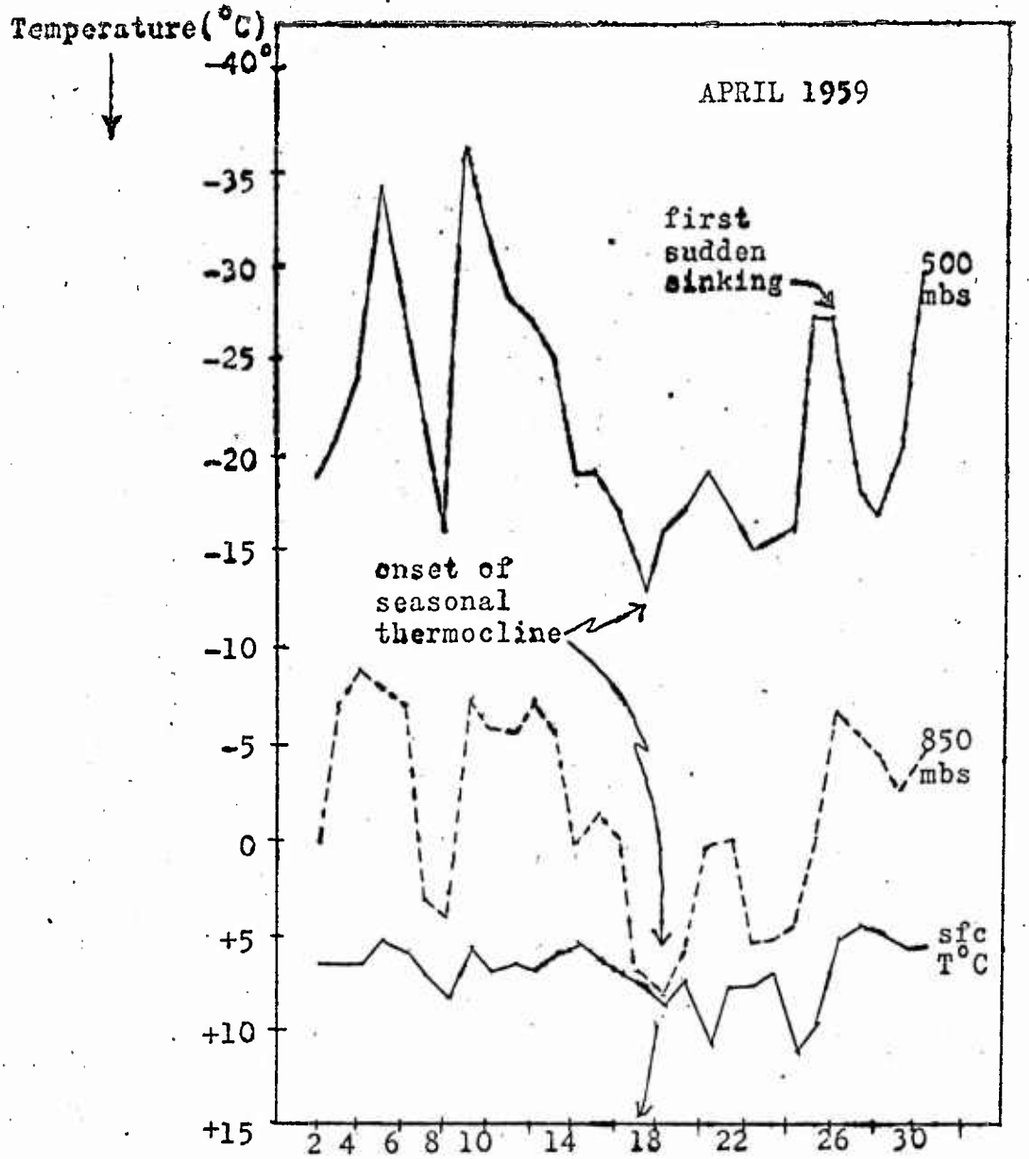

Fig.2 Temperature profiles (0000Z) during the onset of the seasonal thermocline at Ocean Station "P". The 500 mb temperature reached a maximum on 17 April 1959, the date that the seasonal thermocline commenced. The date of maximum temperature can be traced down through the atmospheric layers with appropriate lag. Note that the surface temperature does not reach its maximum value until the thermocline is firmly established.

4. Distribution of Atmospheric Stability During the Onset Month

If we examine the distribution of stability in the inner troposphere during April 1959, the month that the seasonal thermocline commences, we note the following variations in the distribution as described by Clark [2]:

> Prior to the establishment of the thermocline, the over-all picture of the troposphere shows unstable lapses in the lowest layers adjacent to the sea surface with a tendency toward increased stability aloft. However, as the thermocline sets in, the reverse picture is true. Surface inversions are established on 16 April and persist through the onset until 19 April. At the same time the higher atmospheric levels experience a decrease in stability and on the day that the thermocline commences the lower troposphere is composed of two extreme layers; below 3,000 meters we have extremely stable conditions with three inversions appearing while above 3,000 meters unstable conditions dominate. As the surface pressure falls, ascending air and increased instability destroy the surface inversions. During the period that the surface pressure rises, 21 to 24 April, subsidence assists in the temporary re-establishment of surface inversions. On 25 April, the increase in depth of the ocean isothermal layer coincides with an abrupt reversal of the stability distribution aloft. Here we see that the surface inversion has completely disappeared and has been replaced by an unstable layer extending to almost 1500 meters. This unstable layer persists through 28 April, slowly decreasing in depth as middle atmospheric inversions are rapidly established aloft.

Hence we note that during the onset of the thermocline, atmospheric stability prevails, and during the sudden sinking of the mixed layer the reverse picture is true. Since the maintenance of the mixed layer at a greater depth during this sinking period represents very stable conditions in the ocean just below the mixed layer, it appears that the lower atmospheric layers adjacent to the sea are attempting to compensate for the increase in oceanic stability and so maintain a 'balance' of stability conditions at the air-sea

interface. This compensating effect seems to exist throughout the onset month.

Atmospheric stability during the onset months for 1957 and 1958 was analyzed as well, and Showalter Stability Indices [5] were computed on a daily basis and appear in figure 3 in profile form for these months. Unfortunately, the Showalter Stability Index tended to smooth major stability variations and depicted a vertical average, rather than a detailed, analysis of the existing atmospheric conditions. This fact is readily apparent if we compare the profile for April 1959 with the detailed stability cross-section which appears in [2], reproduced here as figure 4. One can observe a tendency toward stable conditions as the thermocline commences and a minimum value does show up on 25 April to accompany the sinking of the mixed layer; on the whole, it was felt that the Stability Index profiles did not represent a sufficiently detailed analysis of the true stability conditions for comparison purposes.

As a matter of interest, daily soundings for April 1959 were compared with the computed Showalter Stability Indices; it was interesting to note that a minimum value of +5 represented the most unstable sounding of the month. A neutrally stable sounding produced a value of +7.7 and the index values increased to a maximum of +20 for the more stable conditions. Showalter developed this index primarily as a thunderstorm forecasting tool for use over land areas, so that it is not surprising to note that our index scale has shifted to higher values when applied over the ocean.

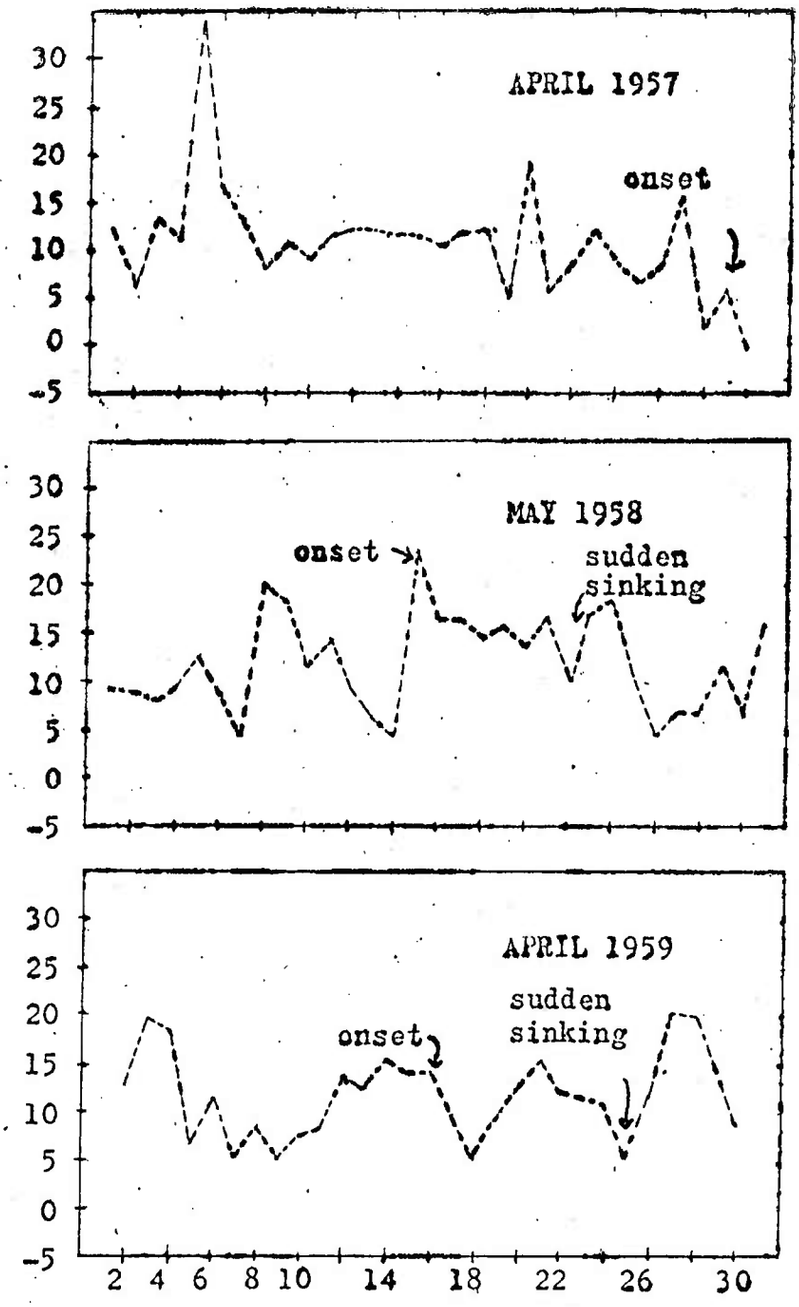

Fig. 3 Showalter Stability Index Profiles accompanying the onset of the seasonal thermocline at Ocean Station "P".

Fig. 3. Distribution of Stability in the Troposphere at Station "P", during April 1959. The dark areas represent inversion layers.

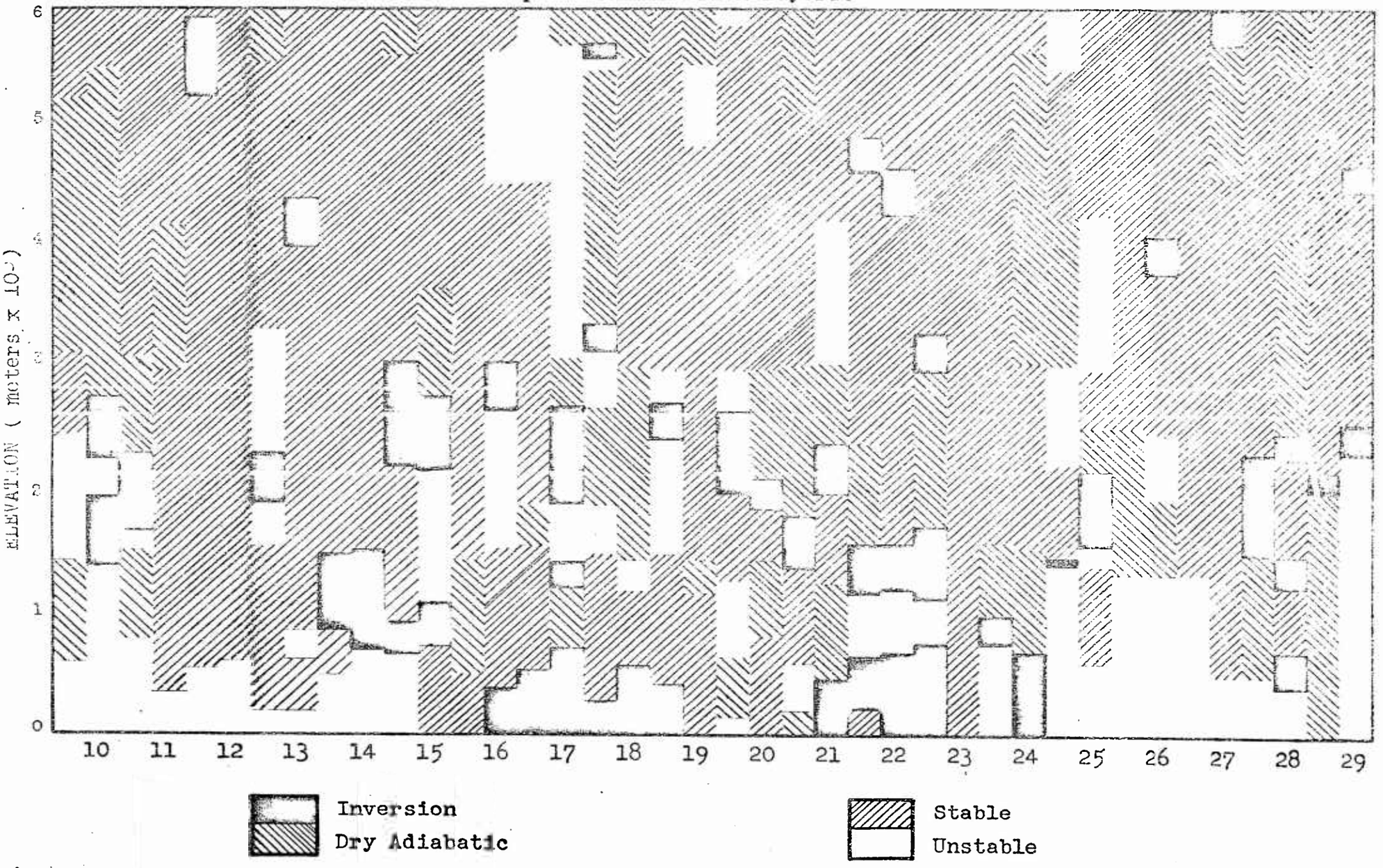

During the course of this investigation, consideration was given to developing a graphical forecasting technique for predicting the temperature difference in the upper 30 meters of the ocean. The Showalter Stability Index was utilized as one of the six basic parameters in lieu of the lapse rate previously used in reference [3]. While the graphical forecasting technique was not included in this paper, it should be mentioned that inclusion of this parameter did not result in as significant a contribution as initially hoped. However, at no time did the index tend to err in the wrong direction.

5. Relative Humidity

In a previous study [2], the author, in discussing the surface relative humidity during the onset of the thermocline in 1959 found:

> It is interesting to note that operations had to cease temporarily during the period 16 to 18 April (coincident with the establishment of the thermocline) due to extreme fog conditions. For a period of six days the lowest relative humidity recorded was 96% with most of the days maintaining a value of 100%. As we approach the 25th of April the relative humidity decreased steadily reaching its lowest value of 70% coincident with the sudden sinking of the thermocline.

In figure 5, the relative humidity at 850 mb is shown for this same month to indicate the distribution of moisture aloft. In 1957 and 1958 as well, the relative humidity is at a maximum value coincident with the establishment of the thermocline; and minimum values are reached when the isothermal layer extends to greater depths. Also, when the actual water vapor content of the atmosphere immediately above station "P" was examined and a level selected where maximum variations in the moisture concentration occurred, it was found that the greatest changes in the concentration of vapor occurred in the layer 850 mb to 700 mb. In reference [2], figure 2 , reproduced here as figure 6, an excellent example of this appears. A decided maximum in the mixing ratio profile occurs on the onset date with a minimum value existing during the sinking of the mixed layer.

Over land, maximum advection of water vapor occurs at 900 mb, [6], and one would be inclined to expect a slightly lower elevation for this same phenomenon over a water surface. However, an analysis of the level of maximum

concentration of, and variations in, the moisture content aloft reveals that over the ocean, at least at station "P", the greatest variation in water vapor content appears to be at a slightly higher altitude, namely, in the vicinity of 850 mb. Frawley and Clark [3], in selecting a forecasting parameter for inclusion in a graphical technique for predicting the temperature distribution in the upper layers of the sea, substituted the 850 mb relative humidity for the surface humidity. Inclusion of this upper-level parameter improved the accuracy of the forecasting technique.

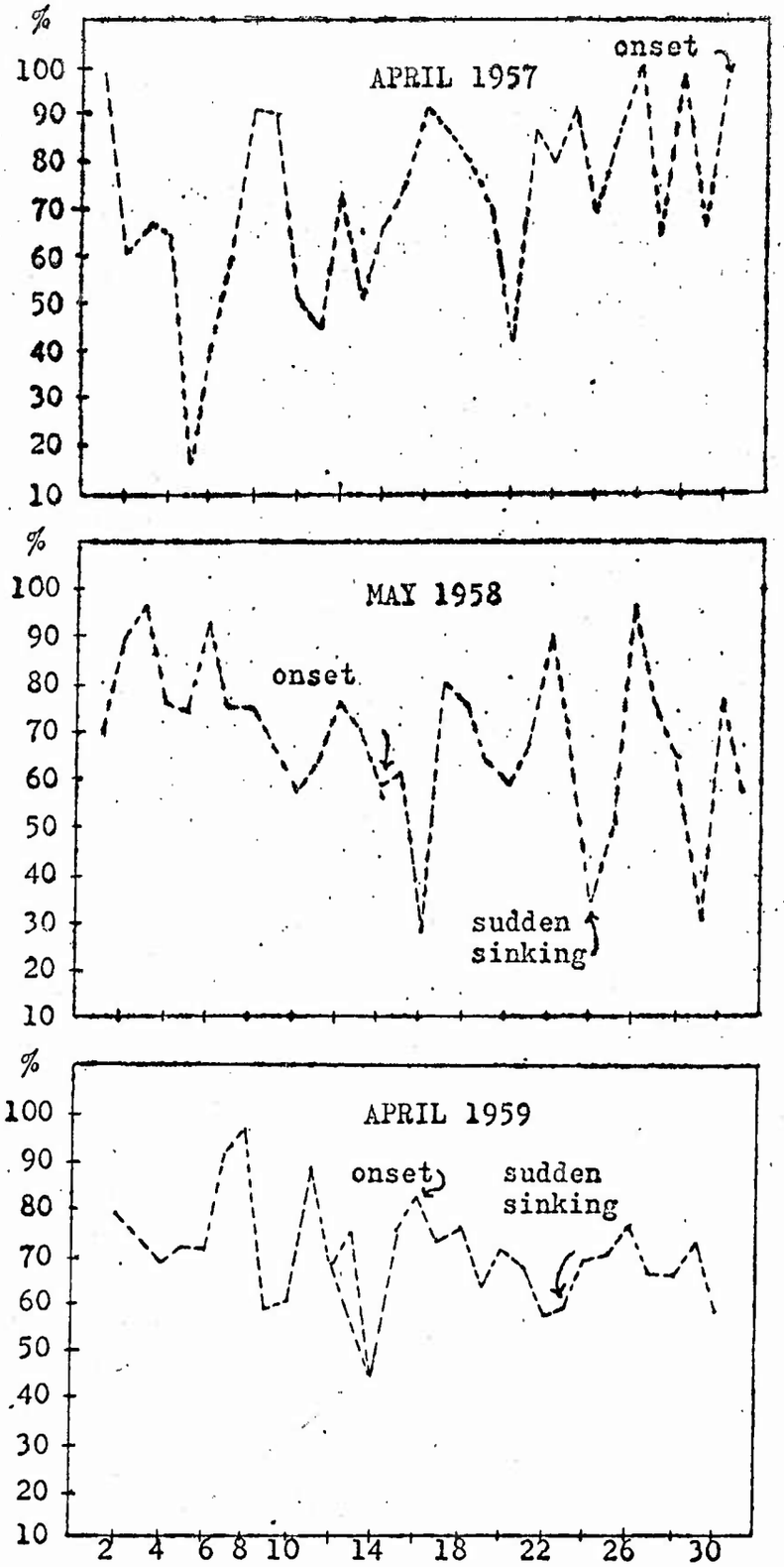

Fig.5 Relative Humidity at 850 mbs(000Z) during the onset of the seasonal thermocline at Ocean Station "P".

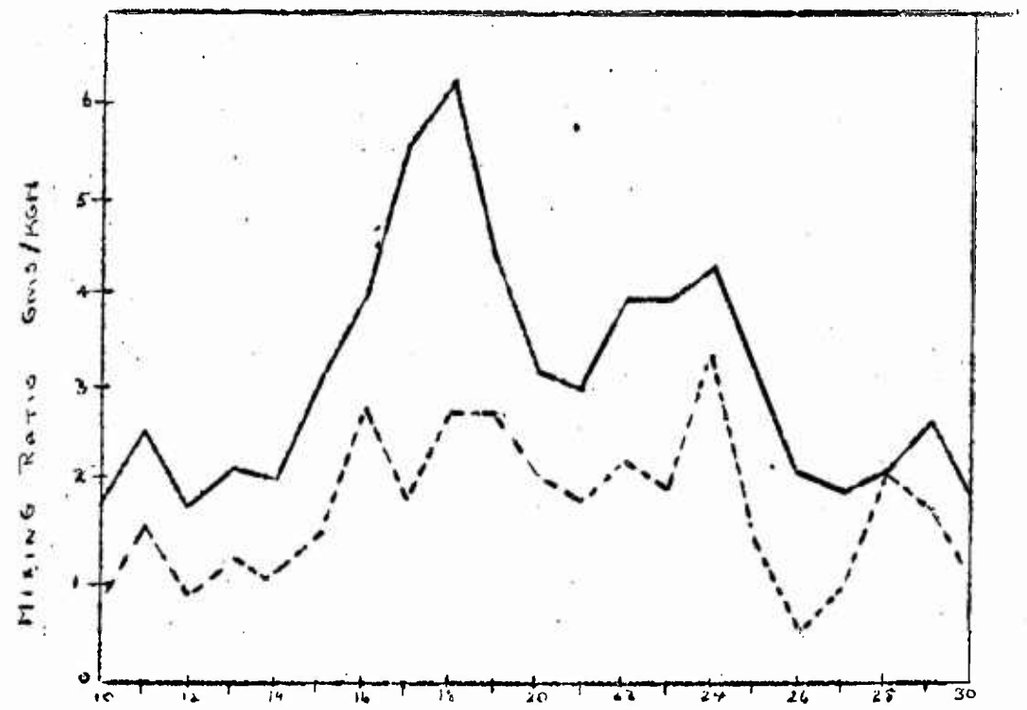

Fig. 6a. Mixing ratio profile (solid-850 mbs; dashed 700 mbs) for 0000Z soundings at Station "P" April 1959.

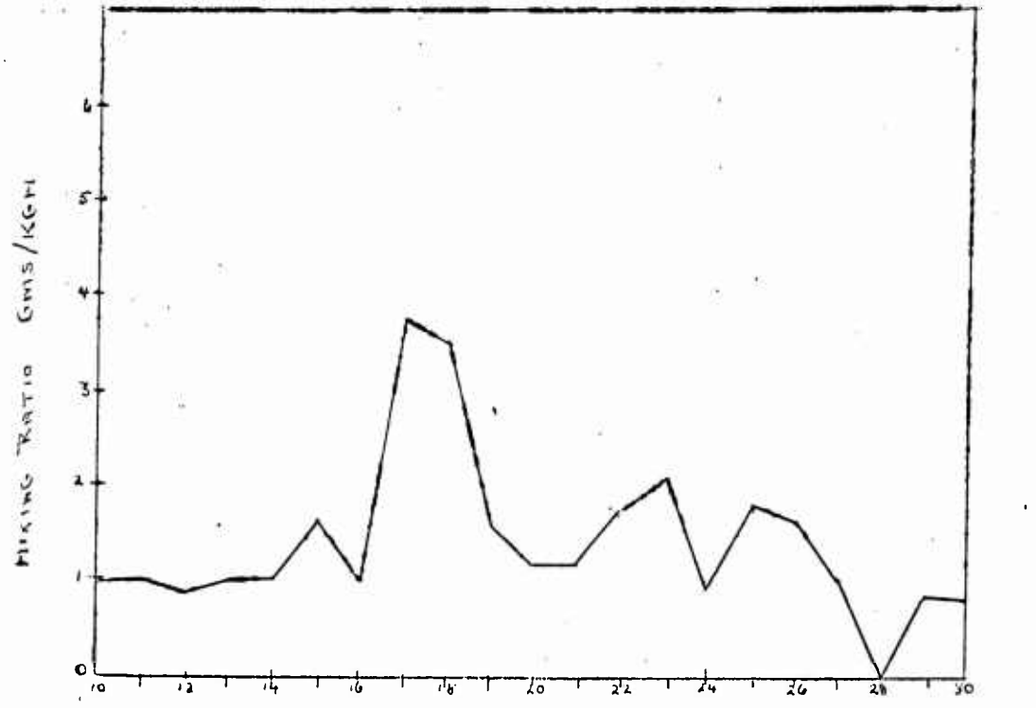

Fig. 6b. Mixing ratio profile (gms/kgm) for the layer 850 mbs to 700 mbs at Station "P", April 1959.

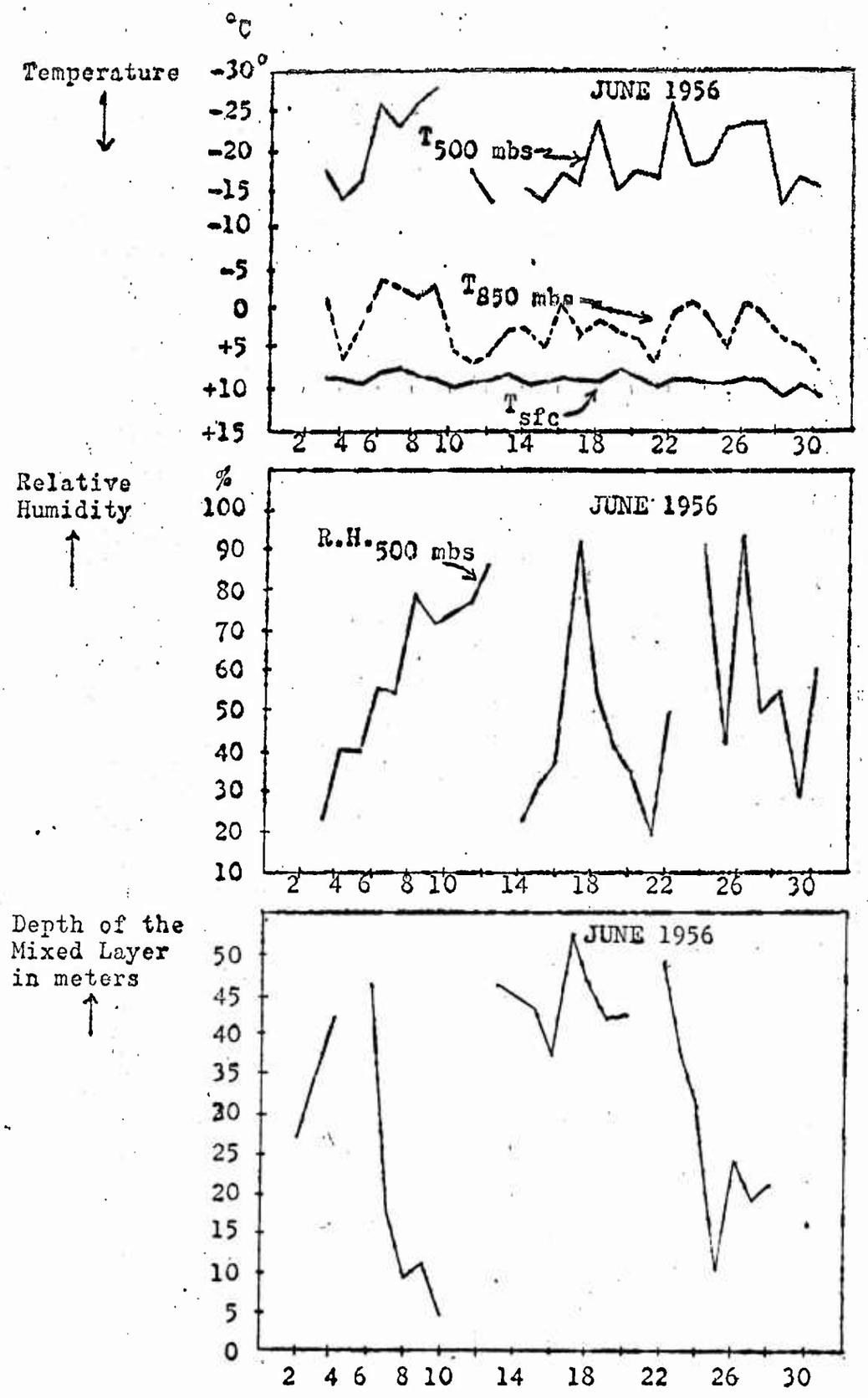

Fig.7 Profiles of Temperature and Relative Humidity at 0300Z are plotted for comparison with the Depth of the Mixed Layer at 0200Z the following day.

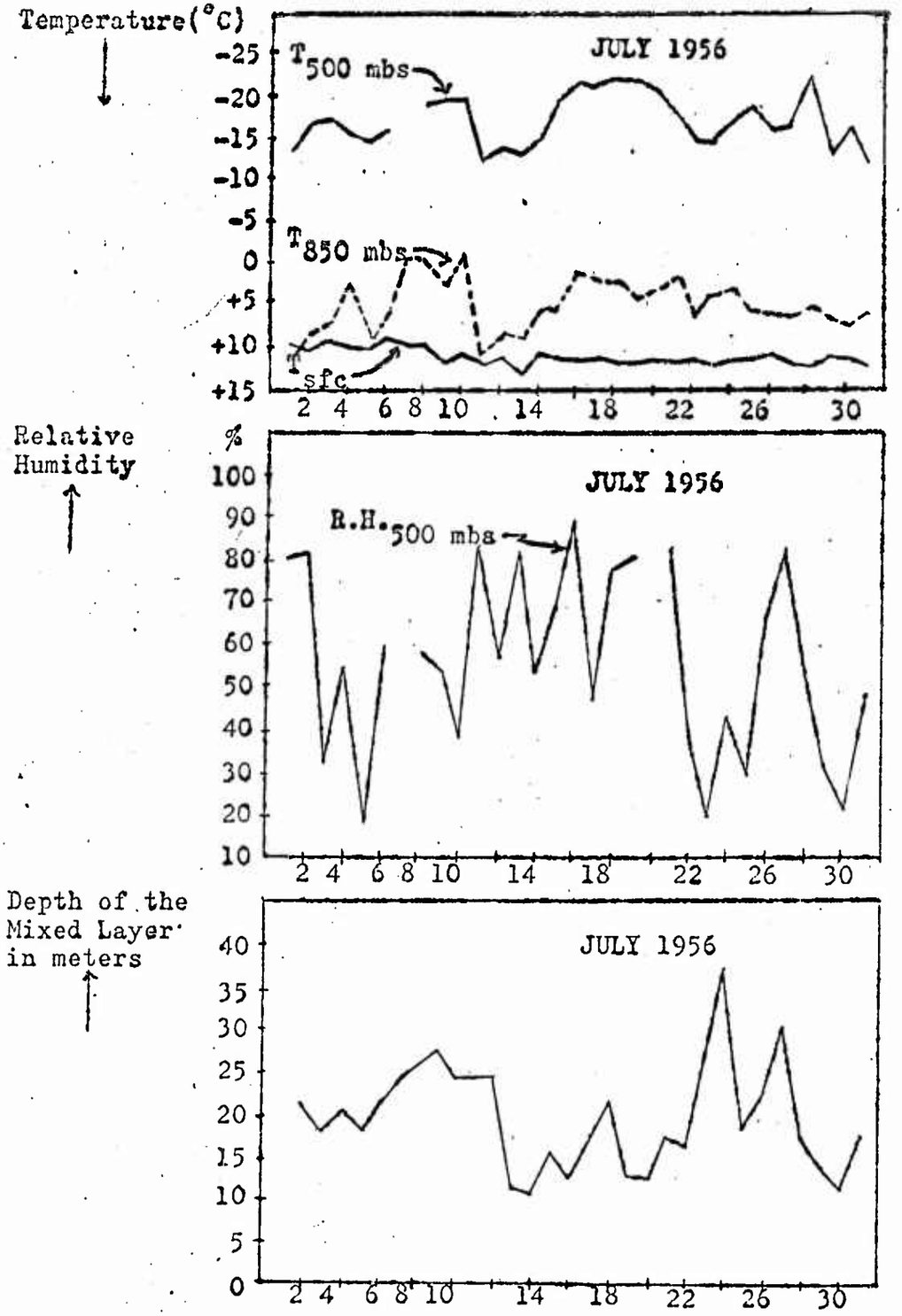

Fig.8 Profiles of Temperature and Relative Humidity at 0300Z are plotted for comparison with the depth of the mixed layer at 0200Z the following day.

6. Tropopause Height and Level of Maximum Winds During the Onset

In figures 9 through 20 the tropopause height, level of maximum winds, and the maximum wind speed aloft have been plotted for the onset months of 1957, 1958 and 1959. For ease of comparison, the mixed layer depth has been plotted separately for each of these months and the actual onset date and first sudden sinking are shown on the respective profiles.

In figure 9 for April 1959, we find that the tropopause has a tendency to reach its maximum elevation during the period that the thermocline sets in (17 April). At the same time, we see that the level of maximum winds and the maximum wind speed aloft, figure 10, experience minimum values on the onset date. However, when the mixed layer undergoes its first sudden sinking on 25 April, we see that the reverse picture is true. While the tropopause is at a minimum height, the level of maximum winds returns to greater heights with an accompanying increase in wind speed aloft. This tendency appears to hold true for the other years examined (figures 12 through 20).

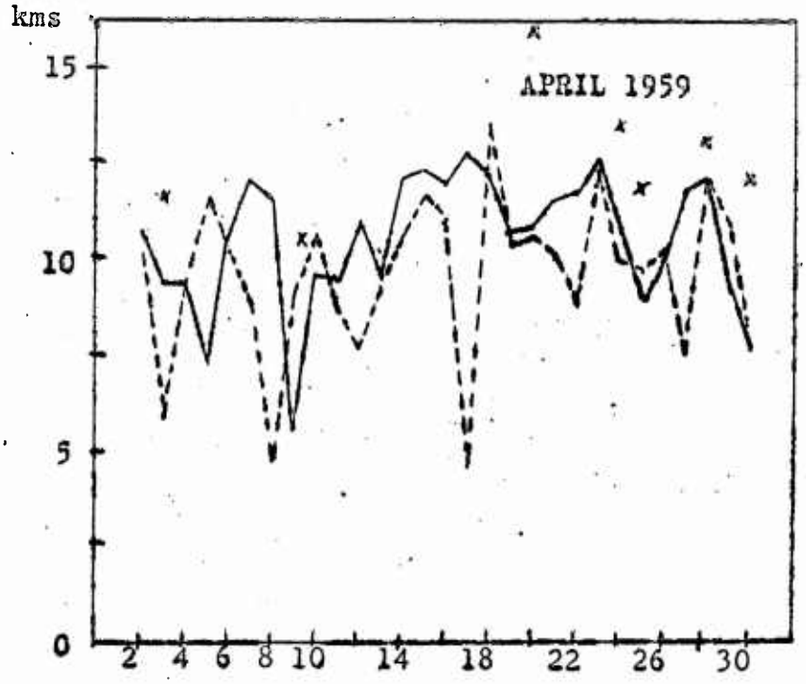

Fig.9 Tropopause height at 0000Z (solid), and Level of Maximum Winds (dashed). x's indicate tropopause #2.

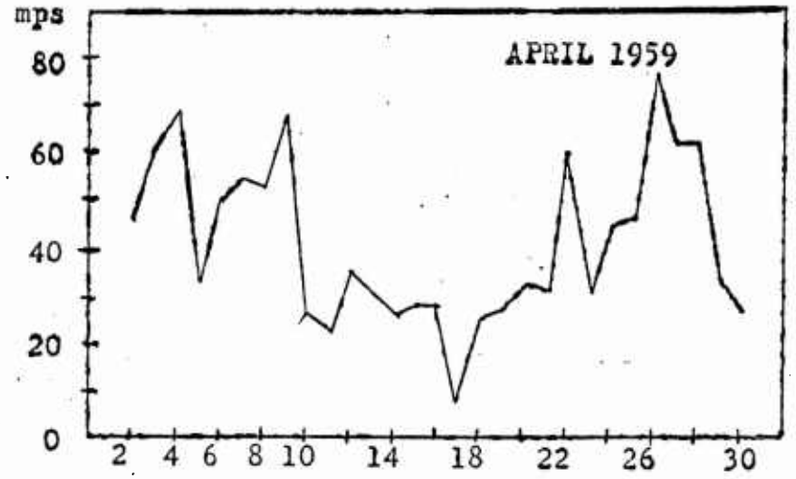

Fig.10 Maximum wind speed aloft at 0000Z during onset of the seasonal thermocline at Ocean Station "P".

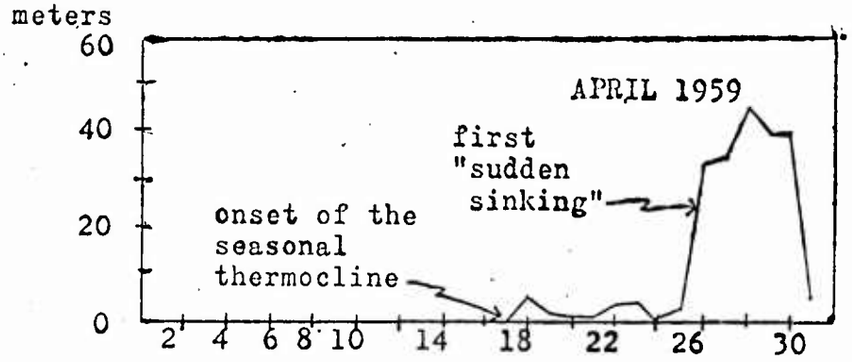

Fig.11 Mixed Layer Depth at 0200Z at Ocean Station "P".

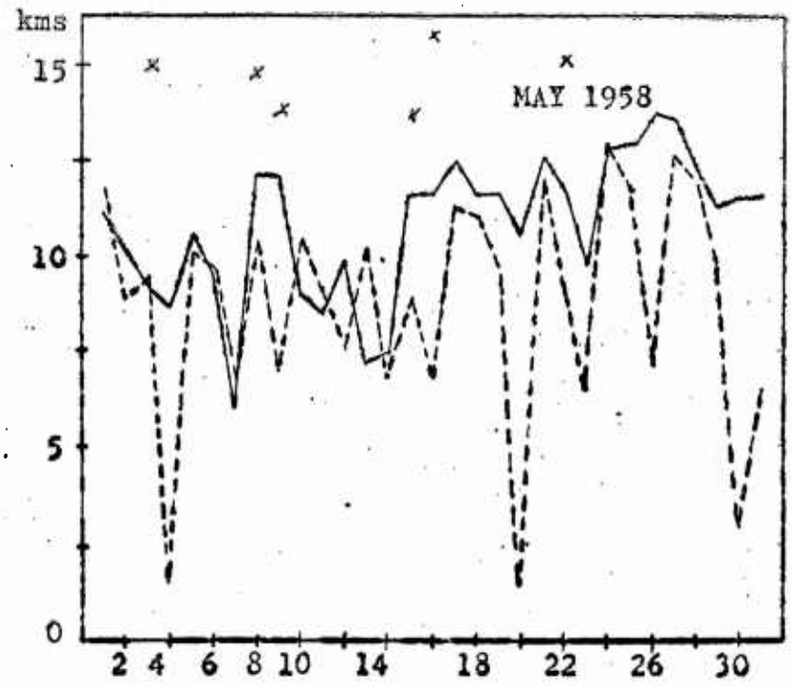

Fig.12 Tropopause height at 0000Z (solid), and Level of Maximum Winds (dashed). x's indicate tropopause # 2.

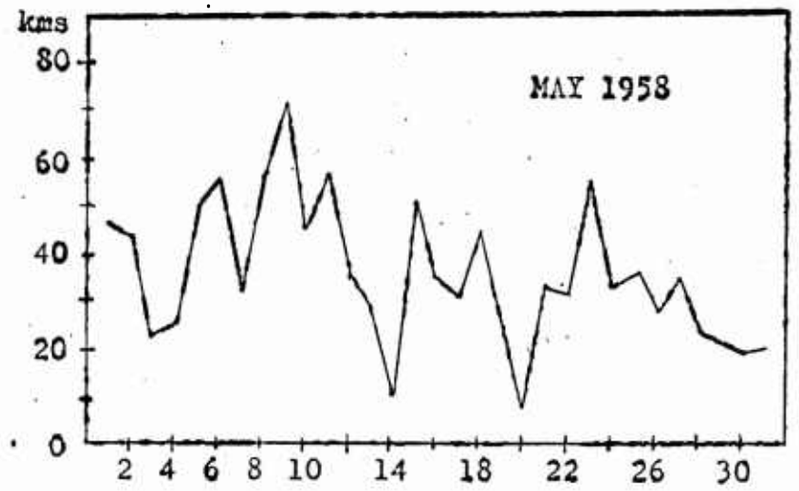

Fig. 13 Maximum wind speed aloft at 0000Z during onset of the seasonal thermocline at Ocean Station "P".

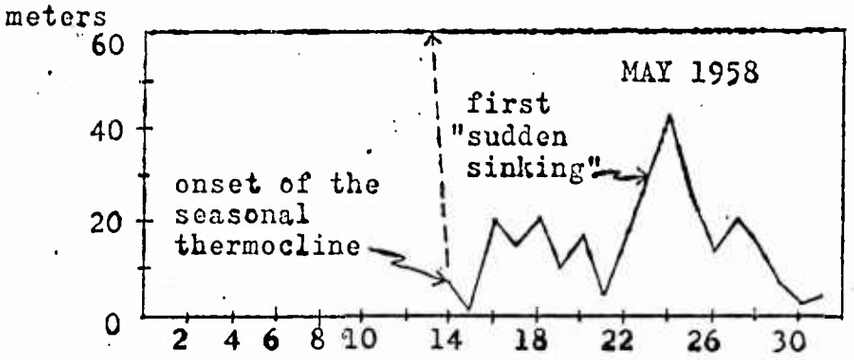

Fig. 14 Mixed Layer Depth at 0200Z at Ocean Station "P".

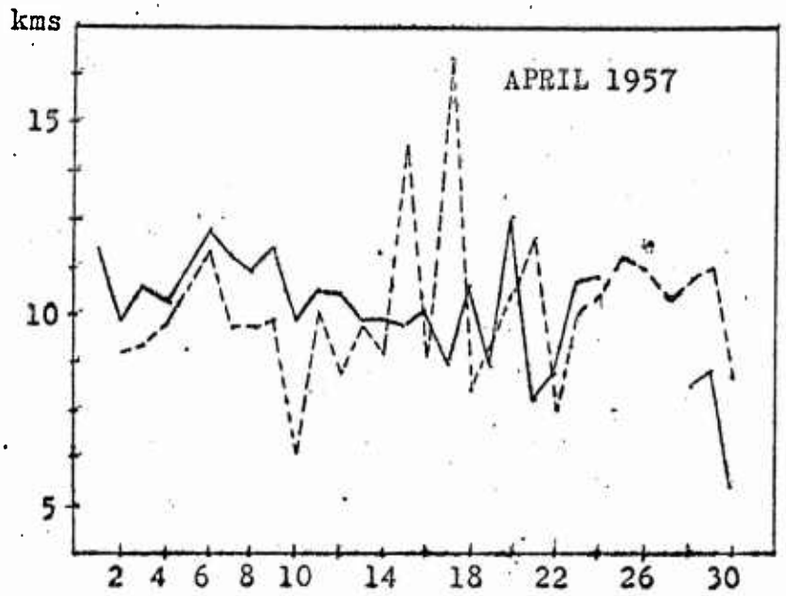

Fig.15 Tropopause height at 0300Z(solid), and Level of Maximum Winds(dashed). x's indicate tropopause #2.

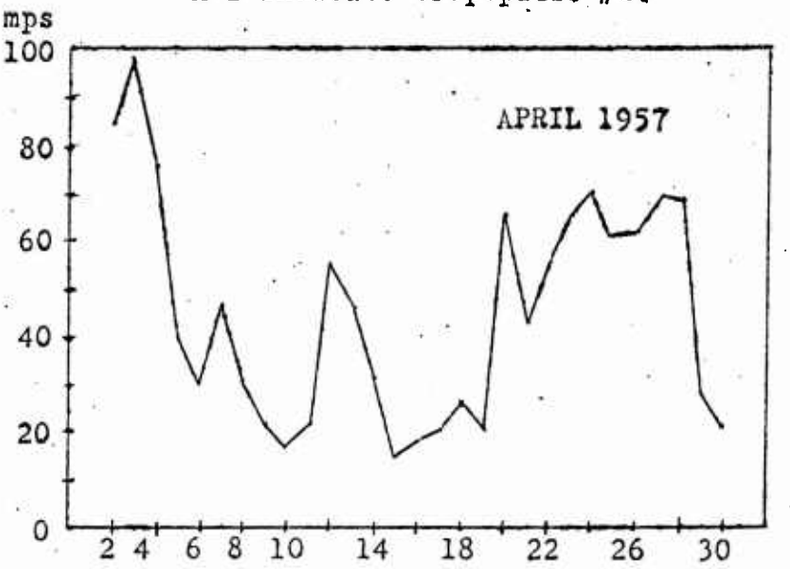

Fig. 16 Maximum wind speed aloft at 0300Z preceding the onset of the seasonal thermocline at Ocean Station "P".

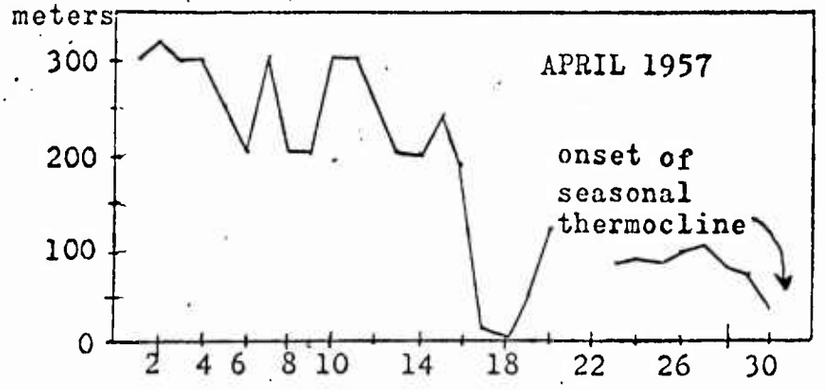

Fig.17 Depth of the Main Thermocline preceding the onset of the Seasonal Thermocline at Station "P".

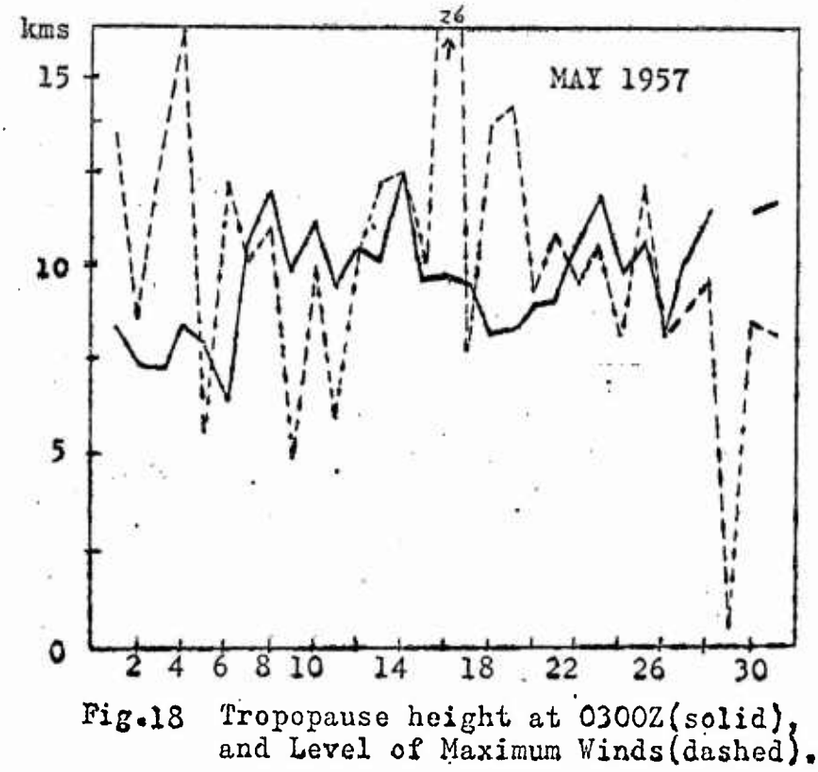

Fig.18 Tropopause height at 0300Z(solid), and Level of Maximum Winds(dashed).

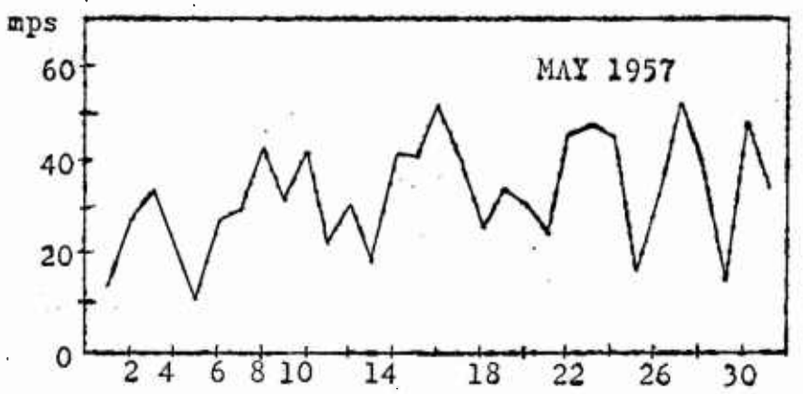

Fig.19 Maximum wind speed aloft at 0300Z following the onset of the seasonal thermocline at Ocean Station "P".

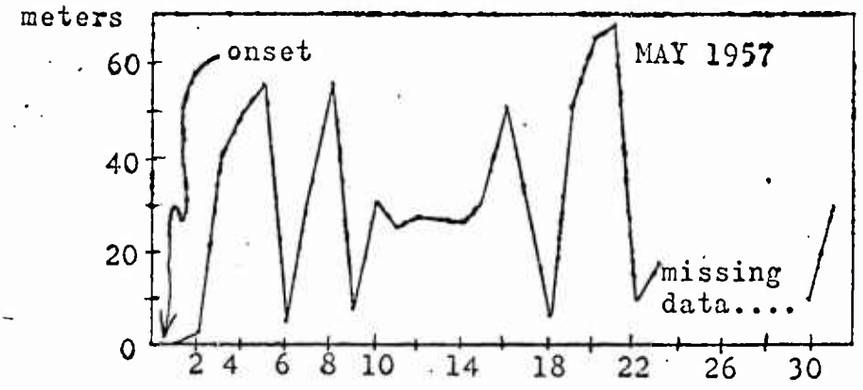

Fig. 20 Mixed Layer Depth at 0300Z at Ocean Station "P".

7. Wind Speed at 6000 Meters

In figure 21, the 0600Z wind speed profile at 6000 meters is shown for the month of June 1958. For ease of comparison, the actual depth of the mixed layer existing at 0200Z on the following day was plotted, utilizing the same scale. With the introduction of this twenty-hour lag we note that the two curves tend to parallel each other fairly well during the first three-quarters of the month. However, it is apparent that the assumption of a constant lag throughout the month cannot be correct, for the two curves are decidedly out of phase during the period 25 June through 27 June. Following this three-day period, the curves again continue in phase until once again, around the 25th through the 27th of the following month, the maximum phase difference occurs. This was the case for all months examined during the four year period 1956 through 1959. Additional months are included as figures 23 through 26.

However, for simplicity, a constant twenty-hour lag was assumed, and the 6000-meter wind speed was correlated with the depth of the mixed layer yielding a correlation coefficient of 0.83 for this particular month. In order to determine whether this rather high correlation existed throughout the balance of the spring and summer months, coefficients were computed for 1956, 1957 and 1958 and are tabulated in Appendix I, Table VI. It should be noted that for the 1959 months where wind speeds at 500 mb were substituted for the 6000-meter winds which were not available for this study, a marked decrease in correlation resulted.

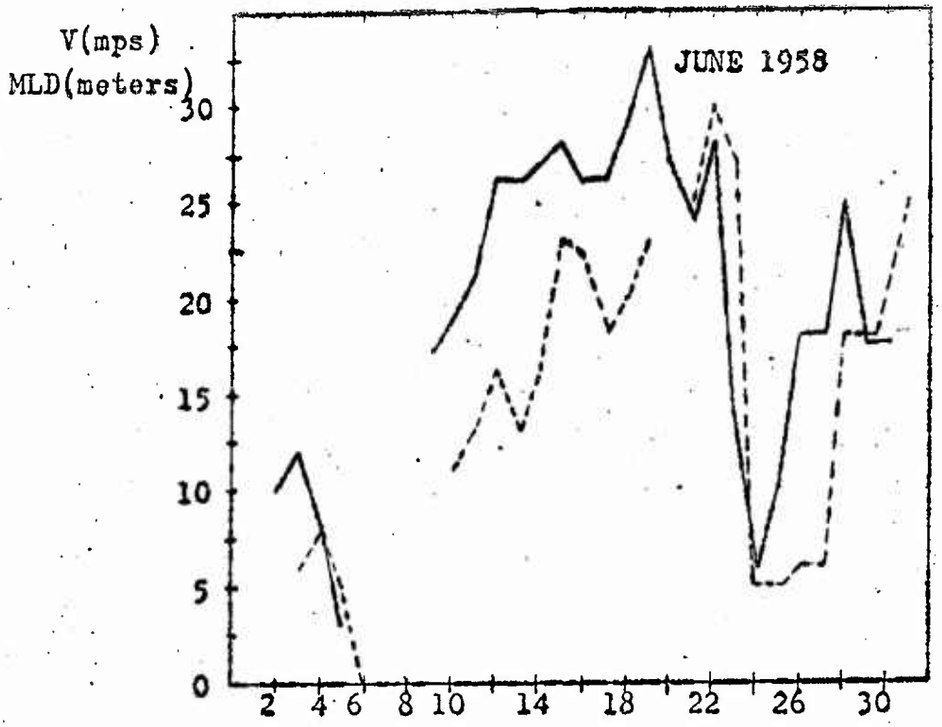

Fig.21 0600Z Wind Speed at 6000 meters(solid) and MLD at 0200Z the following day (dashed). A 20 hour lag is indicated by the profiles.

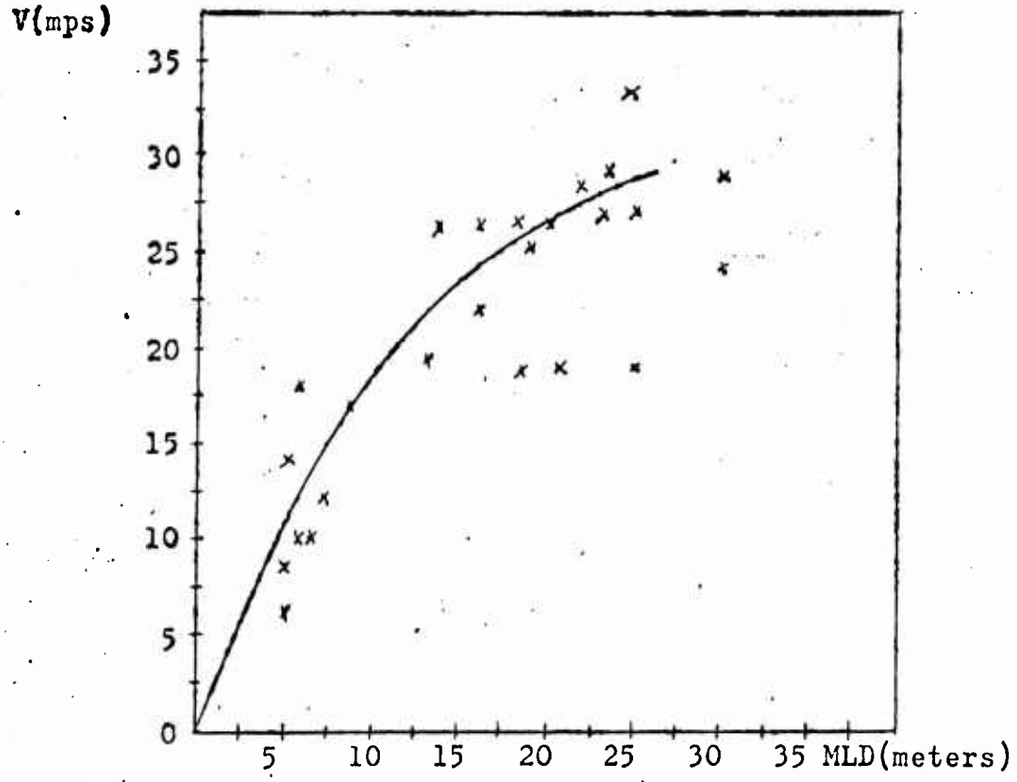

Fig.22 Scatter Diagram suggesting an exponential relationship between the wind speed at 6000 meters, and the depth of the mixed layer at Ocean Station "P".

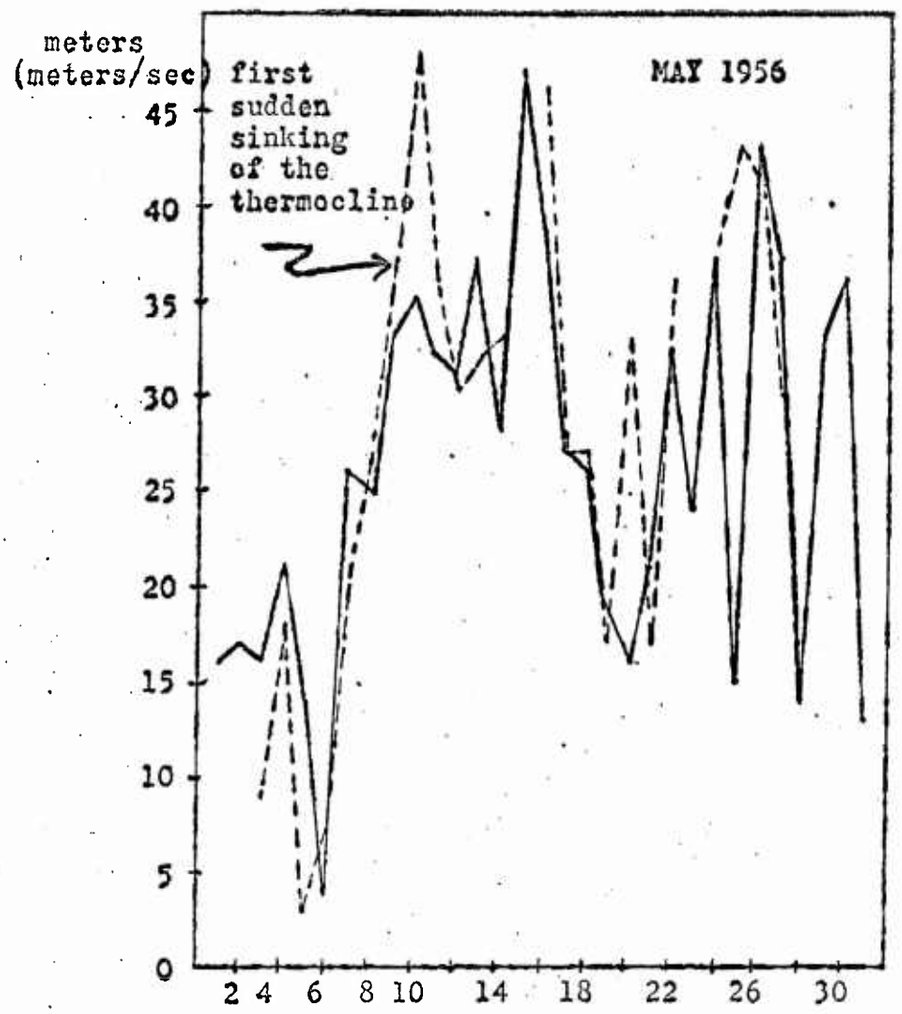

Fig.23 6000 meter wind speed at 0300Z(solid) and depth of the mixed layer at 0200Z (dashed). Correlation coefficient for this month was .73

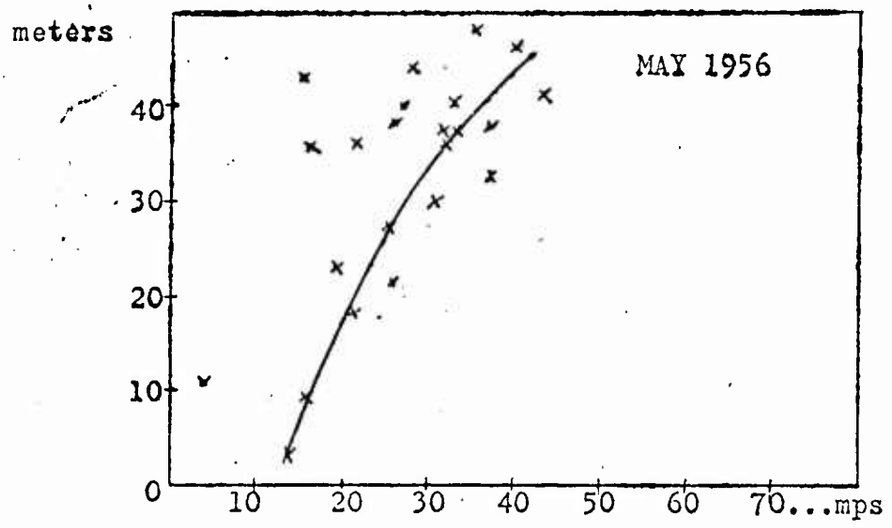

Fig.24 Depth of mixed layer at 0200Z plotted vs 6000 meter wind speed at previous 0300Z.

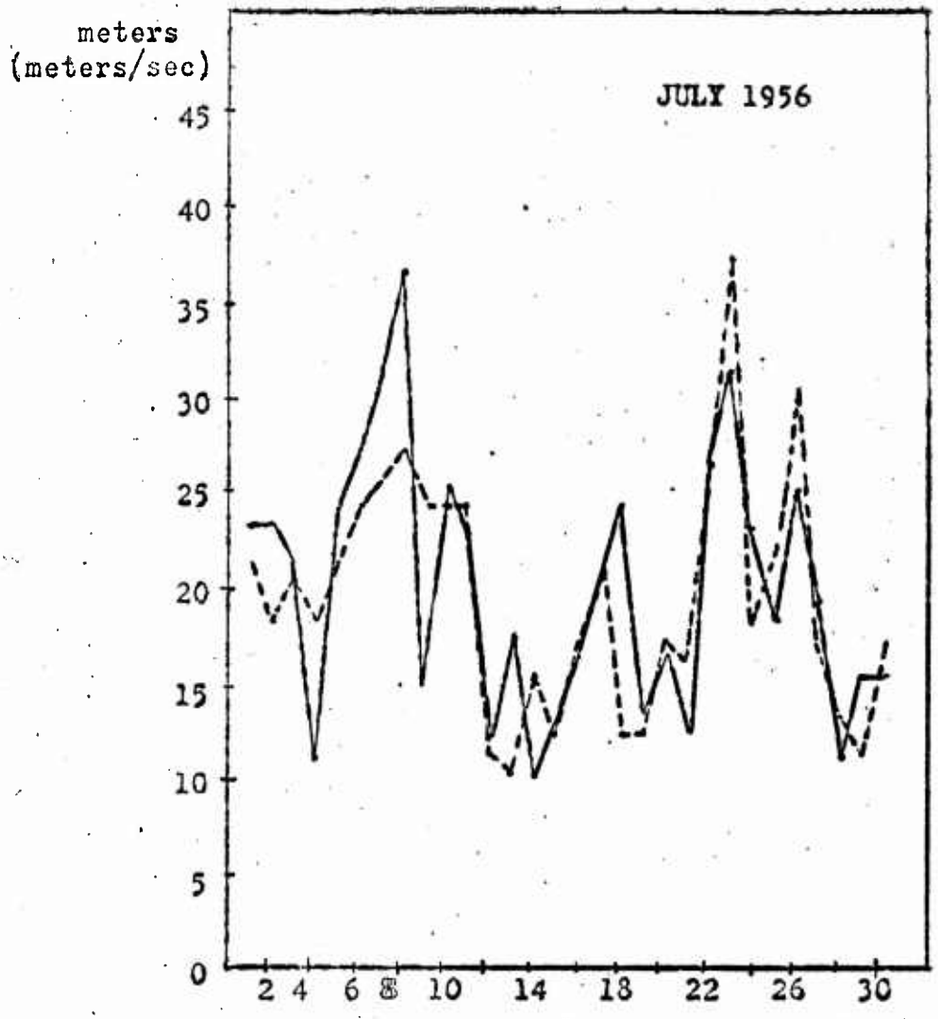

Fig 25 6000 meter wind speed at 0300Z(solid) and depth of the mixed layer at 0200Z (dashed). Correlation coefficient for July 1956 was .70

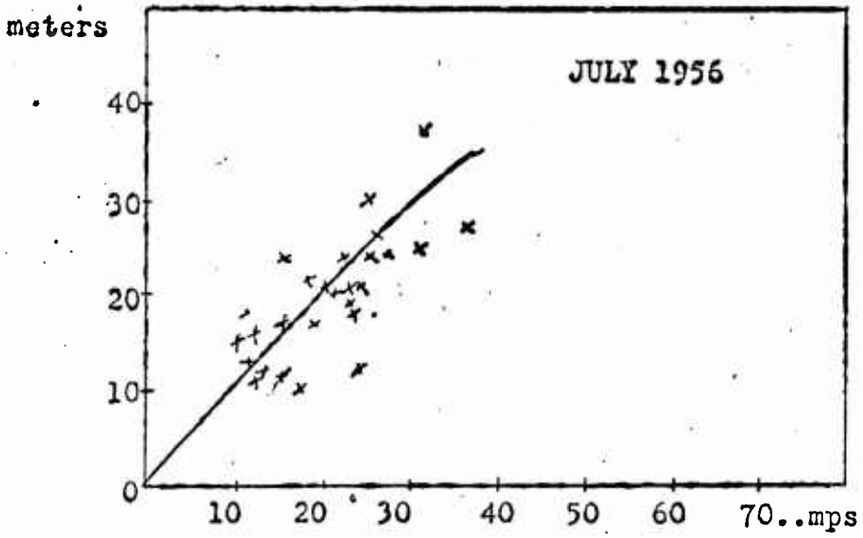

Fig 26 Depth of mixed layer at 0200Z plotted vs 6000 meter wind speed at previous 0300Z.

Surface wind speeds were also correlated with the mixed-layer depth and are included in Table VI for comparison. For all months except two, July 1958 and June 1956, the correlation coefficients for the upper wind speeds were higher. Table VI also illustrates that for both levels, the correlation between wind speed and the depth of the mixed layer decreased as the season progressed. This would suggest that as the thermocline deepened toward the end of the summer months, the effectiveness of the wind as a mixing agent decreased.

8. Development of an Empirical Relationship Between the 6000-Meter Wind Speed and the Depth of the Mixed Layer

The 6000-meter wind speed was plotted against the depth of the mixed layer and the resultant scatter diagram is shown for the month of June 1958 in figure 22. Since the distribution suggested an exponential relationship between the two parameters, the equation of the 'best fit' curve was assumed to be of the form

$$MLD = k_1 \exp(0.1V) \qquad (1)$$

where k_1 is a proportionality factor. When plotted against the wind speed, k_1 turned out to be a linearly-decreasing function of the 6000-meter wind speed and the resultant best-fit straight line may be seen in figure 27. Hence, the final relationship is

$$MLD = e^{0.1V} (2.9-0.056V) \qquad (2)$$

where V represents the 6000-meter wind speed at 0600Z in meters per second and MLD is the depth of the mixed layer in meters at 0200Z of the following day.

Equation (2) was developed on the basis of one month's data only, June 1958, and was tested as a possible twenty-hour empirical prediction formula for all spring and summer months over the four-year period 1956 through 1959. Computed predictions for the depth of the mixed layer were compared with the actual depth existing at 0200Z and the results for each month are tabulated in Appendix I, Table I. The average absolute error for the period analyzed was [illegible] meters.

JUNE 1958

EMPIRICAL SOLUTION FOR PARAMETER k, where 'k' is a decreasing function of wind speed at 6000 meters.

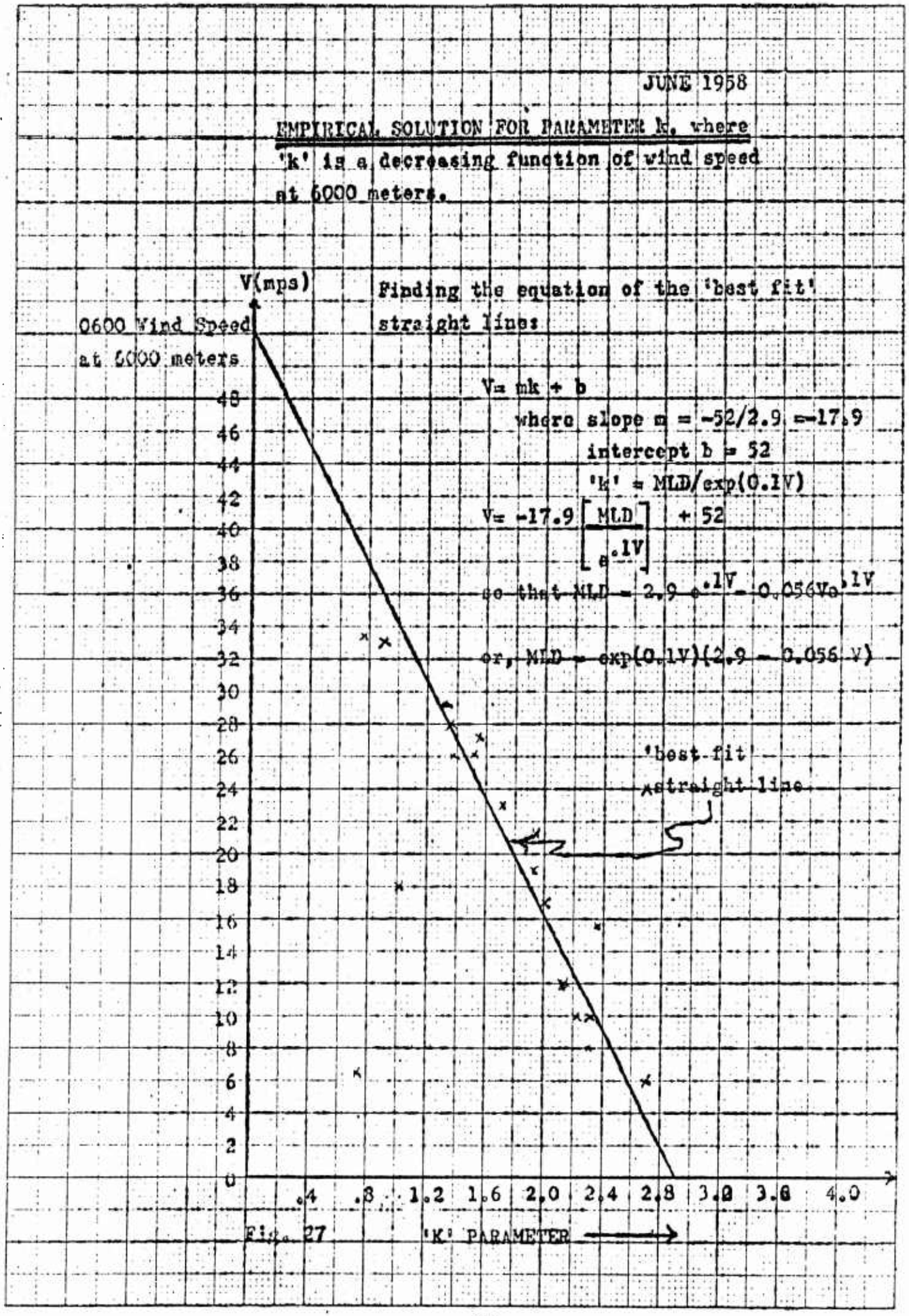

Finding the equation of the 'best fit' straight line:

$V = mk + b$

where slope $m = -52/2.9 = -17.9$

intercept $b = 52$

$'k' = MLD/\exp(0.1V)$

$V = -17.9 \left[\frac{MLD}{e^{.1V}}\right] + 52$

so that $MLD = 2.9\, e^{.1V} - 0.056 V e^{.1V}$

or, $MLD = \exp(0.1V)(2.9 - 0.056\, V)$

'best-fit' straight line

Fig. 27

9. Wind Speed Greater than 70 Knots

When the 6000-meter wind speed exceeded 35 meters per second (approximately 70 knots), the magnitude of the error resulting from equation (2) became excessive for practical purposes. Accordingly, isolated cases for wind speeds exceeding this value were analyzed and appear in scatter-diagram form in figure 28. We note that the distribution suggests an almost-linear relationship between the wind speed and the depth of the isothermal layer, but the best-fit curve appears to be slightly convex toward the right. Hence the equation of the curve was assumed to be of the form

$$V = k_2 e^{mD} \qquad (3)$$

where D represents the depth of the mixed layer in meters, V represents the 0600Z wind speed at 6000 meters in meters per second, and k_2 and m are proportionality factors. Ln V is plotted against the depth of the mixed layer in figure 29; since the resulting distribution is linear, the initial assumption appears to be verified. The mathematical details are delineated in figure 29 and the final equation becomes

$$D = 54.3 \ln V - 161.5 \qquad (4)$$

Computed prediction depths for the isothermal layer were prepared for all cases during the four years where wind speeds were greater than 70 knots and the results appear in Appendix I, Table II. The average absolute error for the entire period analyzed was 3.3 meters.

For Wind Speeds Greater Than 35 meters/sec

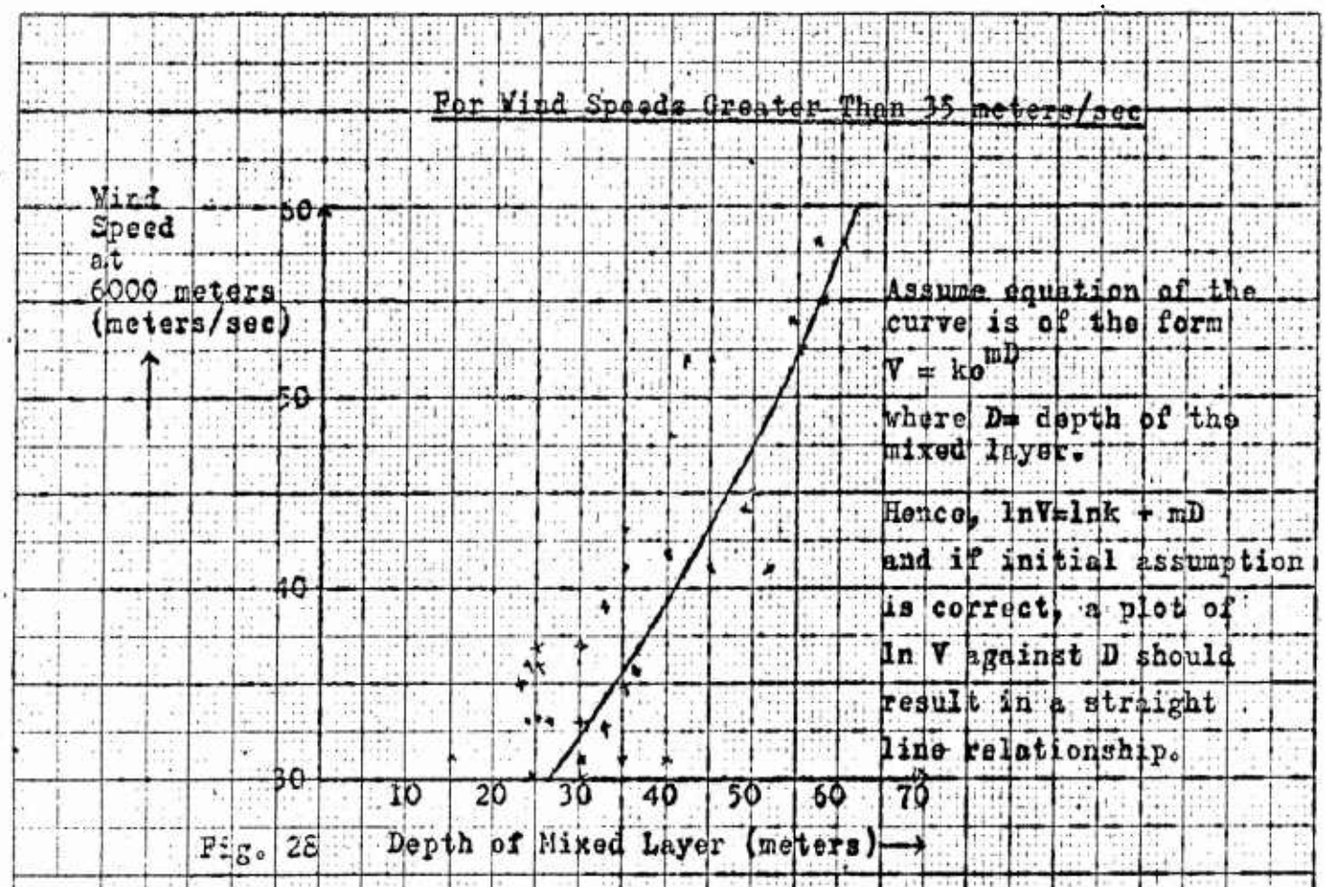

Assume equation of the curve is of the form $V = ko^{mD}$

where D= depth of the mixed layer.

Hence, $\ln V = \ln k + mD$

and if initial assumption is correct, a plot of ln V against D should result in a straight line relationship.

Fig. 28

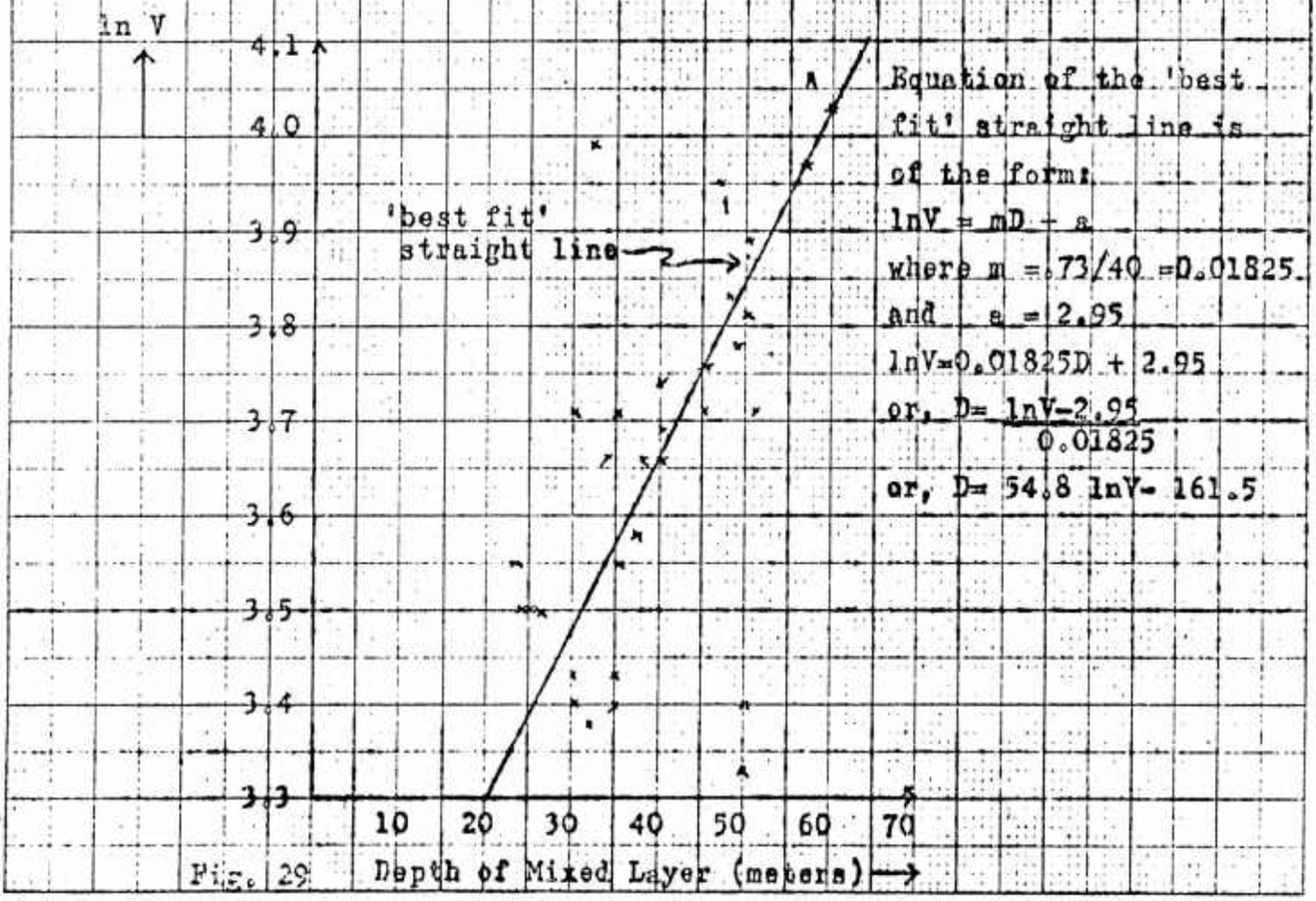

Equation of the 'best fit' straight line is of the form:

$\ln V = mD + a$

where $m = .73/40 = 0.01825$

and $a = 2.95$

$\ln V = 0.01825D + 2.95$

or, $D = \frac{\ln V - 2.95}{0.01825}$

or, $D = 54.8 \ln V - 161.5$

Fig. 29

10. Statement of Hypotheses and the 'Mirror Image' Concept

As a result of this investigation, two basic hypotheses are presented: (1) that the ocean mixed layer and the layer of air in immediate contact with the ocean surface behave as a unit which is affected by meteorological parameters aloft; and (2) that there exists in the upper atmosphere a 'mirror image' level where the fluctuations in wind speed closely depict the oscillation in the depth of the mixed layer.

In presenting these hypotheses, it is definitely not the intention of the author to dispute the fact that surface parameters of sea and air do affect the ocean temperature structure directly below the adjacent layers of the atmosphere. However, it is contended that this layer acts essentially as a buffer affecting the rate of cooling, or the rate of heating, and as such cannot act as a heat source for the underlying waters. Hence, in choosing a basic forecasting parameter for a starting point, the parameter should not be chosen necessarily from this air-sea transition zone.

The profiles and graphs of meteorological parameters such as temperature, wind speed and relative humidity, prepared for various levels in the atmosphere and discussed in the paper, support the first hypothesis. In addition, the mathematical relationship developed between the wind speed aloft and the depth of the mixed layer tends to support hypothesis (2). The possibility of a 'mirror image' level at 6000 meters is a new and rather interesting concept. Evidence of its existence has been demonstrated in the preceding pages, but a 'cause and effect' relationship

between the wind speed at this level and the depth of the mixed layer has been carefully avoided. On the contrary, it is proposed that these two levels are responding similarly to some external triggering action or energy impulse, possibly incoming solar radiation acting on the stratosphere.

11. Conclusions and Recommendations

The scatter-diagrams, empirical formulae developed, and the tested predictions based on the concept of an atmospheric level responding similarly as the depth of the mixed layer, all tend to support the conclusion that a 'mirror-image' of the mixed-layer depth does indeed exist in the atmosphere at an altitude of 6000 meters. It is recommended, however, that in order to derive greater forecasting accuracy from utilization of this upper-air synoptic phenomenon, additional research be undertaken to determine the exact magnitude of the time-lag encountered.

It is further concluded that surface meteorological parameters indicate to a greater extent what <u>has</u> happened to the thermal structure in the upper ocean layers, rather than what <u>will</u> happen, and hence should not necessarily be selected as forecasting parameters. In addition, a more accurate determination of the vertical extent of the layer of air and the ocean mixed layer, which act as a unit, should be attempted.

Finally, since the 850-mb relative humidity would appear to be a more representative forecasting parameter than the surface relative humidity, it is strongly recommended that continued research be conducted in order to derive an empirical relationship between the vertical distribution of atmospheric water vapor and the temperature distribution in the surface layers of the ocean immediately below.

BIBLIOGRAPHY

1. Laevastu, T., Factors Affecting the Temperature of the Surface Layer of the Sea, Societas Scientiarum Fennica, Commentationes Physico-Mathematicae XXV, Helsinki, 1960

2. Clark, M.J., An Investigation into Climatological Changes in the Lower Atmosphere Coinciding with the Onset of the Oceanic Thermocline at Station "P", U.S. Naval Postgraduate School, unpublished manuscript, 1960

3. Frawley, M.J., and Clark, M.J., An Objective Method for Forecasting the Temperature Variation between the Surface and Thirty Meters at Ocean Station "P" for the month of April 1959, U.S. Naval Postgraduate School, unpublished manuscript, December 1960

4. Serebreny, S.M., Wiegman, E.J., and Hadfield, R.G., A Study of Jet Stream Conditions in the Northern Hemisphere During Spring, United States Navy Weather Research Facility, Pan American World Airways, Inc., Technical Report No. 7, San Francisco, June 1958

5. Showalter, A.K., A Stability Index for Thunderstorm Forecasting, Bulletin of the American Meteorological Society, June 1953, Vol 34, No. 6

6. ----------, An Objective QPF system using Warm Advection, National Weather Analysis Center, Office Memorandum 27-60, March 1960

APPENDIX

TABLE I

Computed predictions for the depth of the mixed layer using the forecasting formulae MLD=exp(0.1V) (2.9-0.056V) for V<35 meters/sec; and MLD=54.8 lnV - 161.5 for V≥35 meters/sec, where V=6000-meter wind speed.

Day of Month	6000-m Wind Speed at 0300Z (meters/sec)	Forecast MLD for 0200Z (meters)	Actual MLD at 0200Z (meters)	Forecast MLD-Actual MLD (meters)
May 1956				
1	16	--	M	--
2	17	--	M	--
3	16	10	9	1
4	21	14	18	-4
5	14	8	3	5
6	4	3	7	-4
7	26	26	21	5
8	25	26	27	-1
9	33	35	37	-2
10	35	35	48	-13
11	32	30	36	-6
12	31	28	30	-2
13	37	37	32	5
14	28	29	33	-4
15	52	--	--	--
16	40	41	46	-5
17	27	27	27	0
18	26	27	27	0
19	19	13	17	-4
20	16	10	33	-23
21	21	14	17	-3
22	32	30	36	-6
23	24	--	--	--
24	37	37	38	-1
25	15	10	43	-33
26	43	44	41	3
27	37	37	30	7
28	14	--	--	--
29	33	35	40	-5
30	36	35	M	--
31	13	--	M	--

Average error = 4.3 meters (ignoring 20th & 25th)

TABLE I (Cont'd)

Day of Month	6000-m Wind Speed at 0300Z (meters/sec)	Forecast MLD for 0200Z (meters)	Actual MLD at 0200Z (meters)	Forecast MLD-Actual MLD (meters)
Jun 1956				
1	18	--	M	--
2	26	26	27	-1
3	33	35	34	1
4	31	28	42	-14
5	M	--	M	--
6	23	18	46	-28 *
7	16	10	17	-7
8	5	4	9	-5
9	10	8	11	-3
10	8	6	4	2
11	M	--	--	--
12	M	--	--	--
13	0	0	46	-46 *
14	M	--	--	--
15	28	29	43	-14
16	36	35	37	-2
17	17	12	52	-40 *
18	17	12	46	-34 *
19	26	26	42	-12
20	34	36	42	-6
21	M	--	--	--
22	28	29	49	-20 *
23	31	28	37	-9
24	31	28	31	-3
25	14	8	10	-2
26	21	14	24	-10
27	18	13	19	-6
28	19	13	21	-8
29	M	--	--	--
30	11	8	16	-8

Average error = 9.5 meters

*Excluding 5 days, formula didn't work; average error = 6.2 m

TABLE I (Cont'd)

Day of Month	6000-m Wind Speed at 0300Z (meters/sec)	Forecast MLD for 0200Z (meters)	Actual MLD at 0200Z (meters)	Forecast MLD-Actual MLD (meters)
Jul 1956				
1	23	18	21	-3
2	23	18	18	0
3	21	14	19	-5
4	11	9	18	-9
5	24	19	21	-2
6	27	27	25	2
7	31	28	26	2
8	36	35	27	8
9	15	10	24	-14
10	25	26	24	2
11	22	18	22	4
12	12	10	11	-1
13	17	12	10	2
14	10	8	14	-6
15	13	11	12	-1
16	16	10	17	-7
17	20	14	21	-7
18	24	19	12	7
19	13	11	12	-1
20	16	10	17	-7
21	12	10	16	-6
22	26	26	26	0
23	31	28	36	-8
24	23	18	18	0
25	18	12	22	-10
26	25	26	30	-4
27	19	13	16	-3
28	11	9	12	-3
29	15	10	11	-1
30	15	10	16	-6
31	*M	M	--	--

*M= missing data

Average error = 4.3 meters

TABLE I (Cont'd)

Day of Month Aug 1956	6000-m Wind Speed at 0300Z (meters/sec)	Forecast MLD for 0200Z (meters)	Actual MLD at 0200Z (meters)	Forecast MLD-Actual MLD (meters)
1	8	6	8	-2
2	12	10	14	-4
3	21	14	18	-4
4	21	14	20	-6
5	18	13	20	-7
6	8	--	M	--
7	10	8	13	-5
8	4	3	3	0
9	5	4	6	-2
10	6	5	0	4
11	3	3	0	2
12	5	4	3	1
13	6	5	3	2
14	14	8	9	-1
15	17	12	9	3
16	17	12	12	0
17	11	8	20	-12
18	9	8	24	-16
19	23	18	17	1
20	49	51	18	33 *
21	31	28	18	10
22	40	40	17	23 *
23	30	25	21	4
24	23	18	24	-6
25	42	42	24	18
26	32	30	32	-2
27	30	25	27	-2
28	42	42	27	15
29	42	42	31	11
30	33	35	33	2
31	24	19	31	-12

*Average error = 5.4 meters, excluding 2 days marked *

TABLE I (Cont'd)

Day of Month Jul 1957	6000-m Wind Speed at 0300Z (meters/sec)	Forecast MLD for 0200Z (meters)	Actual MLD at 0200Z (meters)	Forecast MLD-Actual MLD (meters)
1	5	4	45	-41
2	18	12	40,51	-39
3	22	18	53	-35
4	29	23	30	-7
5	23	18	30	-12
6	26	27	35	-8
7	14	8	23	-15
8	12	10	10	0
9	9	--	M	--
10	25	26	30	-4
11	24	19	20	-1
12	M	--	M	--
13	10	8	8	0
14	7	6	6	0
15	14	8	6	2
16	14	8	11	-3
17	7	6	10	-4
18	10	10	14	-4
19	26	25	15	10
20	21	14	15	-1
21	30	25	28	-3
22	29	23	20	3
23	35	34	31	3
24	29	23	20	3
25	18	12	20	-8
26	34	33	30	3
27	31	29	35	-6
28	17	--	M	--
29	24	19	25	6
30	--	--	--	--
31	--	--	--	--

Average error 7 July through 29 July = 3.3 meters

TABLE I (Cont'd)

Day of Month Aug 1957	6000-m Wind Speed at 0300Z (meters/sec)	Forecast MLD for 0200Z (meters)	Actual MLD at 0200Z (meters)	Forecast MLD-Actual MLD. (meters)
1	7	--	M	--
2	M	--	--	--
3	11	10	12	-2
4	20	14	20	-6
5	19	16	28	-12
6	40	40	28	12
7	33	35	35	0
8	19	16	33	-17
9	17	12	30	-18
10	10	8	7	1
11	6	4	5	-1
12	12	10	11	-1
13	8	7	14	-7
14	18	12	20	-8
15	8	--	M	--
16	6	4	4	0
17	6	4	4	0
18	7	6	5	1
19	14	8	5	3
20	11	10	13	3
21	12	10	7	3
22	38	36	33	3
23	30	26	30	-4
24	27	27	25	2
25	8	7	10	-3
26	7	6	5	1
27	M	--	--	--
28	15	10	13	-3
29	14	8	14	-6
30	23	18	22	-4
31	19	16	24	-8

Average error = 4.8 meters. (ignoring 8th & 9th, average error = 3.[illegible] meters)

TABLE I (Cont'd)

Day of Month May 1958	6000-m Wind Speed at 0600Z (meters/sec)	Forecast MLD for 0200Z (meters)	Actual MLD at 0200Z (meters)	Forecast MLD-Actual MLD (meters)
13	10	6	7	-1
14	15	8	4	4
15	31	28	20	8
16	23	17	15	2
17	21	14	20	-6
18	23	17	10	7
19	10	6	17	-11
20	4	3	5	-2
21	12	7	15	-8
22	21	14	30	-16
23	52	54	45	9
24	14	8	25	-17
25	24	18	15	3
26	23	17	20	-3
27	19	12	15	-3
28	10	6	7	-1
29	10	6	3	3
30	13	7	4	3
31	M	--	M	--

Average error = 5.4 meters

TABLE I (Cont'd)

Day of Month Jun 1958	6000-m Wind Speed at 0600Z (meters/sec)	Forecast MLD for 0200Z (meters)	Actual MLD at 0200Z (meters)	Forecast MLD-Actual MLD (meters)
1	M	--	--	--
2	10	6	6	0
3	12	7	7	0
4	8	5	5	0
5	3	3	0	3
6	M	--	--	--
7	M	--	--	--
8	M	--	--	--
9	17	11	11	0
10	19	12	13	-1
11	21	14	16	-2
12	26	19	14	5
13	26	19	16	3
14	27	27	24	3
15	28	21	22	-1
16	26	19	18	1
17	26	19	20	-1
18	29	23	23	0
19	33	29	25	4
20	27	27	25	2
21	24	18	30	-12
22	28	21	26	-5
23	14	8	5	3
24	6	5	5	0
25	10	6	6	0
26	18	12	6	6
27	18	12	18	-6
28	25	18	18	0
29	18	13	20	-7
30	18	13	25	-12

Average error = 3.0 meters

TABLE I (Cont'd)

Day of Month Jul 1958	6000-m Wind Speed at 0600Z (meters/sec)	Forecast MLD for 0200Z (meters)	Actual MLD at 0200Z (meters)	Forecast MLD-Actual MLD (meters)
1	17	11	25	-14
2	21	14	16	-2
3	27	27	25	2
4	39	38	35	3
5	23	17	14	3
6	14	8	12	-4
7	15	8	5	3
8	12	7	15	-8
9	11	7	18	-11
10	24	18	15	3
11	M	--	--	--
12	16	10	25	-15
13	8	5	10	-5
14	11	7	13	-6
15	4	3	2	1
16	6	5	15	-10
17	23	17	23	-6
18	18	12	15	-3
19	29	23	28	-5
20	39	38	34	4
21	25	18	22	-4
22	18	12	20	-8
23	35	32	30	2
24	26	19	25	-6
25	M	--	--	--
26	M	--	--	--
27	23	17	23	-6
28	28	27	25	2
29	33	29	26	3
30	54	56	27	29 *
31	15	8	33	-25 *

*Average error = 5.5 meters, excluding 2 days marked *

TABLE I (Cont'd)

Day of Month Aug 1958	6000-m Wind Speed at 0600Z (meters/sec)	Forecast MLD for 0200Z (meters)	Actual MLD at 0200Z (meters)	Forecast MLD-Actual MLD (meters)
1	30	25	30	-5
2	25	18	28	-10
3	22	16	35	-19
4	18	12	25	-13
5	M	--	--	--
6	M	--	--	--
7	M	--	--	--
8	15	8	32	-24 *
9	12	7	35	-28 *
10	41	41	41	0
11	5	4	0	4
12	23	17	30	-13
13	41	41	36	5
14	39	38	38	0
15	31	25	30	-5
16	23	17	35	-18
17	31	31	30	1
18	M	--	--	--
19	M	--	--	--
20	14	8	40	-32 *
21	29	24	32	-8
22	25	18	30	-12
23	27	27	45	-18
24	40	40	40	0
25	18	12	25	-13
26	19	13	25	-12
27	18	12	25	-13
28	36	36	37	-1
29	39	38	40	-2
30	42	42	40	2
31	16	10	15	-5

Average error = 10.3 meters *(excluding 8,9,20th, average error = 7.9 meters)

TABLE II

Computed predictions for the depth of the mixed layer using the forecasting formula MLD=54.8 lnV - 161.5 for wind speeds greater than 35 meters/sec.

Date	6000-m Wind Speed At 0600Z (meters/sec)	Forecast MLD for 0200Z (meters)	Actual MLD at 0200Z (meters)	Forecast MLD-Actual MLD (meters)
1956 May 13	37	37	32	5
16	40	41	46	-5
24	37	37	38	-1
26	43	44	41	3
27	37	37	30	7
Jun 16	36	35	37	-2
Aug 20	49	51	18	33 *
22	40	40	17	23 *
28	42	42	27	15
29	42	42	31	11
1957 Jul 23	35	34	30	4
26	34	33	29	4
Aug 7	33	35	35	0
22	38	36	32	4
1958 May 23	52	54	45	9
Jul 4	39	38	35	3
20	39	38	34	4
23	35	32	30	2
30	54	56	27	29 *
Aug 10	41	41	41	0
13	41	41	35	6
14	39	38	38	0
24	40	40	40	0

Date	6000-m Wind Speed At 0600Z (meters/sec)	Forecast MLD for 0200Z (meters)	Actual MLD at 0200Z (meters)	Forecast MLD-Actual MLD (meters)
1958 Aug 28	36	36	37	-1
29	39	38	40	-2
30	42	42	40	-2
Sep 4	35	32	35	-3
6	43	44	45	1
18	46	48	48	0
20	41	41	50	9
21	58	60	57	3
22	44	45	49	4
23	41	41	45	4
24	45	46	50	4
25	49	51	50	1
1959 Apr 28	52	54	53	1
May 7	43	44	41	3
10	54	56	55	1
19	37	30	28	2
Aug 4	39	38	34	4
6	39	38	36	2
17	39	38	42	4

Average error 3.3 meters.

*Excluding 3 dates formula failed to predict correctly

TABLE III

Summary of mean error (forecast MLD-actual MLD) for months tested during the period 1956 through 1958.

	1956		1957		1958	
Month	No. of days tested	Mean error (meters)	No. of days tested	Mean error (meters)	No. of days tested	Mean error (meters)
May	24	4.3	--	--	18	5.4
June	23	6.2	--	--	26	3.0
July	30	4.3	26	3.3	28	5.5
August	30	5.4	27	3.8	26	7.9
Total	87	5.0	53	3.5	98	5.4

Mean error for the period 1956 through 1958 was 4.9 meters

TABLE IV

Statistical Analysis of daily errors (forecast MLD - actual MLD) for the testing period 1956 through 1958. Total number of days = 258

Error $\leq$ (meters)	No. of days occurrence	Percentage of total days tested
2	82	32
3	117	45
4	138	54
5	154	60
6	174	68
7	185	72
8	198	77
9	201	78
10	207	81
11	210	82
12	220	85
13	225	87
14	229	89
15	232	90

TABLE V

Monthly means and standard deviations for the 6000-meter wind speed and the depth of the mixed layer (MLD).

	Mean Wind Speed (mps)	Standard Deviation of Wind Speed	Mean MLD (meters)	Standard Deviation of MLD	Correlation Coefficient
1956					
May	27.0	9.5	29.0	12.0	.73
Jun	21.4	9.6	30.3	14.3	.47
Jul	19.8	6.5	19.1	6.3	.70
Aug	21.0	12.0	16.0	9.7	.79
1958					
May	18.6	10.5	14.8	10.9	.71
Jun	19.9	7.9	15.6	8.4	.82
Jul	21.9	11.0	18.3	8.0	.48
Aug	25.7	10.2	30.4	9.0	.58
1959					
Apr	21.7	14.2	16.8	17.9	.83
May	*20.8	12.1	25.9	12.6	*.38
Jun	*14.9	6.5	27.2	21.9	*.35
Aug	*19.5	10.6	35.4	11.8	*.10

*6000-meter wind speed data not available for these months. Substitution of the 500-mb wind speed resulted in decreased correlation between the two parameters.

TABLE VI

Correlation coefficients (r)** for the depth of the mixed layer against (1) surface wind speed, and (2) 6000-meter wind speed.

	1956		1958		1959	
	Surface	Aloft	Surface	Aloft	Surface	Aloft
Apr	---	---	---	---	---	---
May	.39	.73	.26	.71	.36	.38*
Jun	.74	.47	.74	.82	.43	.35*
Jul	.24	.70	.61	.48	---	---
Aug	.73	.79	.40	.58	.00	.10*

*6000-meter data not available. Substitution of the 500-mb wind speed resulted in a greatly decreased correlation between the parameters.

$$r = \frac{\Sigma(x-\bar{x})(y-\bar{y})}{n\, S_x\, S_y}$$

where $S_x = \sqrt{\frac{\Sigma(x-\bar{x})^2}{n}}$

and $S_y = \sqrt{\frac{\Sigma(y-\bar{y})^2}{n}}$